Science of the Total Environment 937 (2024) 173363

Contents lists available at ScienceDirect

Science of the Total Environment

journal homepage: www.elsevier.com/locate/scitotenv

Projections of the start of the airborne pollen season in Barcelona (NE Iberian Peninsula) over the 21st century

Marta Alarcón [a,*], María del Carmen Casas-Castillo [b], Raül Rodríguez-Solà [c], Cristina Periago [a], Jordina Belmonte [d,e]

[a] Departament de Física, EEBE, Universitat Politècnica de Catalunya - BarcelonaTech, Eduard Maristany 16, 08019 Barcelona, Spain
[b] Departament de Física, ESEIAAT, Universitat Politècnica de Catalunya - BarcelonaTech, Colom 1, 08222 Terrassa, Spain
[c] Departament de Física, ETSEIB, Universitat Politècnica de Catalunya - BarcelonaTech, Diagonal 647, 08028 Barcelona, Spain
[d] Institut de Ciència i Tecnologia Ambientals (ICTA-UAB), Universitat Autònoma de Bellaterra, 08193 Bellaterra, Spain
[e] Departament de Biologia Animal, Biologia Vegetal i Ecologia, Facultat de Biociències, Universitat Autònoma de Barcelona, 08193 Bellaterra, Spain

HIGHLIGHTS

- A forecast model of the pollen season start combined with climate scenarios was applied.
- Long-term pollination start dates were predicted for 6 pollen types in Barcelona.
- All projections resulted in an advancement of the pollen season over the 21st century.
- More than 80 % of the trends obtained for these advancements were significant.
- The more pessimistic the scenario, the greater the forecasted advancement.

GRAPHICAL ABSTRACT

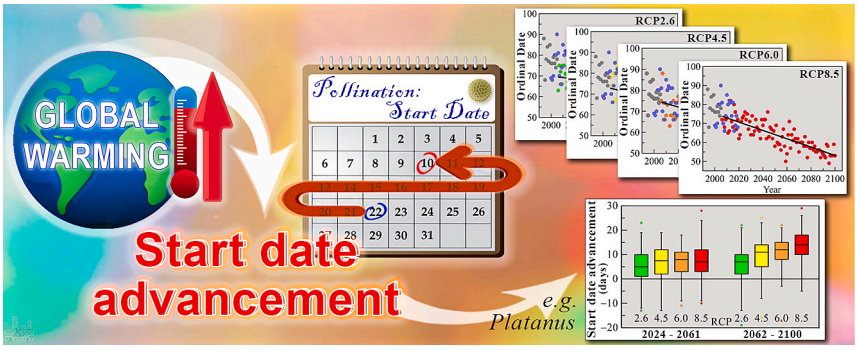

ARTICLE INFO

Editor: Anastasia Paschalidou

Keywords:
Climate change
Forecast
Temperature projections
Start pollination
Pollen prediction
Allergenic pollen

ABSTRACT

The effects of global warming are numerous and recent studies reveal that they can affect the timing of pollination. Temperature is the meteorological variable that presents a clearer relationship with the start of the pollination season of most of the observed airborne pollen taxa. In Catalonia, in the last fifty years, the average annual air temperature has increased by +0.23 °C/decade, and the local warming has been slightly higher than the one on a global scale. Projections point to an increase in temperature in the coming decades, which would be more marked towards the middle of the century.

To analyse the effect of the increase in temperature due to global warming on the starting date of pollen season in Barcelona, a forecasting model has been applied to a set of projected future temperatures estimated by the European RESCCUE project. This model, largely used in the literature, is based on determining the thermal needs of the plant for the pollen season to begin. The model calibration to obtain the initial parameters has been made by using 20 years of pollen data (2000–2019), and the model effectiveness has subsequently been tested through an internal evaluation over the period of the calibration and an external evaluation on 4 years not included in the

* Corresponding author.
E-mail addresses: marta.alarcon@upc.edu (M. Alarcón), m.carmen.casas@upc.edu (M.C. Casas-Castillo), raul.rodriguez@upc.edu (R. Rodríguez-Solà), cristina.periago@upc.edu (C. Periago), jordina.belmonte@uab.cat (J. Belmonte).

https://doi.org/10.1016/j.scitotenv.2024.173363
Received 8 February 2024; Received in revised form 16 May 2024; Accepted 17 May 2024
Available online 23 May 2024

calibration (2020−2023). The mean bias error in the internal calibration ranged between −0.4 and − 0.6 days, and between +0.5 and − 8.3 in the external one, depending on the taxon. The results of the application of the model to the temperature projections over the 21st century point to a progressive advancement in the pollination dates of several pollen types abundant in the city, allergenic most of them. These advances ranged, at the end of the century, between 15 and 27 days, depending on the climate model, for the scenario of the highest concentrations (RCP8.5) and between 7 and 12 days for the emissions stabilization scenario (RCP4.5).

1. Introduction

Airborne pollen concentrations in a given area depend on many factors, basically the surrounding vegetation, meteorology (Cariñanos et al., 2022; Alarcón et al., 2023), and atmospheric transport patterns that can bring the pollen from distant regions (Izquierdo et al., 2011, 2017; Bogawski et al., 2019; Alarcón et al., 2022; Bayr et al., 2023). Among the meteorological variables, the most influential are temperature and precipitation (Majeed et al., 2018; Schramm et al., 2021). In the city of Barcelona, it has been shown that precipitation can both reduce the airborne pollen levels by a washing out effect, or increase them in the following spring after abundant rain in the winter months prior to flowering (Rodríguez-Solà et al., 2022). On the other hand, temperature is the primary factor influencing the growth and development of plants, the flowering intensity, and therefore the pollen concentration, and the timing of the pollen season (Tang et al., 2016; Recio et al., 2018; Ziska et al., 2019; Adams-Groom et al., 2022). Furthermore, an increase in temperature can result in a higher content of allergenic load in pollen grains (Ahlholm et al., 1998; Ariano et al., 2010; Oh, 2022). The rate of the phenological development of plant species increases linearly as a function of cumulative degrees of daily air temperature above a thermal threshold for which it is effective (Laaidi, 2001). As a consequence, global warming and other alterations caused by climate change can affect pollen production and seasonality. In southern Germany, an earlier start and end date for pollination, as well as an increase in the pollen load on tree species, were observed, together with negative correlations between flowering start dates and spring temperatures, especially at high altitudes (Rojo et al., 2021). Menzel (2000) showed that in Europe there has been a general 6-day advance in the flowering of some species over the second half of the past century. Fitter and Fitter (2002) evidenced an increase of 4–5 days in the length of the flowering of different plant species in Great Britain during the decade 1990–1999 compared to the previous four decades. Similar results have been found for elm and birch pollen seasons over the last three decades of the 20th century in several European cities (Emberlin et al., 2002, 2007). Ariano et al. (2010) observed a progressive increase in the duration of the pollen seasons for Urticaceae (+85 days), olive (+18 days), and cypress (+18 days), with an overall advance of their start dates in western Liguria (Italy) between 1981 and 2007. In Southern Spain, Ruiz-Valenzuela and Aguilera (2018) found, for a period of 23 years, a positive trend in pollen concentration and duration for tree species, but a decrease, both in intensity and duration, for herbaceous species. Similar changes have also been found in other areas of the planet: an advance in flowering of about 6 days *per* decade in Seoul (Korea) for the major trees with allergenic pollen (Lee et al., 2021). Ziska et al. (2019) obtained an increase of 0.9 days *per* year in the duration of the pollen season and significant correlations between the increase in minimum and maximum temperature and the annual concentration of various allergenic pollens with data from 17 stations in the Northern Hemisphere. Other recent studies corroborate this influence of global warming on the annual concentration and timing of pollen (Adams-Groom et al., 2022; Anderegg et al., 2021; Bruffaerts et al., 2018; Büntgen et al., 2022; De Weger et al., 2021; Gehrig and Clot, 2021; Hoebeke et al., 2018; Piotrowska-Weryszko et al., 2021). However, there are other factors, also due to human activity, that influence variations in the annual pollen integral, such as changes in land use. In the south of the Iberian Peninsula, a relative decrease in the concentration of pollen from native vegetation (*Quercus* and *Plantago*) and an increase in pollen from cultivated or reforested species (*Olea* and *Pinus*) has been observed (López-Orozco et al., 2023).

Different models that predict the parameters of airborne pollen (start, end, duration and peak of the pollen season) have been developed, most of them based on statistical methods (Stach et al., 2008; Rodríguez-Rajo et al., 2009; Kasprzyk and Walanus, 2010). More recently, Eulerian atmospheric transport models are used to simulate and forecast the pollen season (Sofiev et al., 2006; Sofiev et al., 2013; Sofiev, 2019; Adamov and Pauling, 2023; Sicard et al., 2021). Neural networks and other machine learning algorithms have also been used to predict airborne pollen dynamics and fungal spore concentrations (Grinn-Gofron and Strzelczak, 2008; Valencia et al., 2019; Cordero et al., 2020; Lops et al., 2020; Oh, 2022; Picornell et al., 2024). Predicting the start date of the pollen season is particularly important to alert the sensitive population well in advance so that they can take preventive measures. To this end, some models focus on thermal forcing while others studies are based on the distinction between the cooling stage, using chill units, and the heat accumulation stage, in growing degree hours, from hourly meteorological data (Garcia-Mozo et al., 2000; Luedeling et al., 2021). Several studies predict the onset date based on multiple regression with meteorological variables (Laaidi et al., 2003; Zhang et al., 2015; Oh, 2022). Other authors have used process-based models (Chuine et al., 1999; Garcia-Mozo et al., 2009) considering variables such as temperature, photoperiod and water availability on the time of flowering and long-time series of phenological data of the studied location. One of the most used models for predicting the start date is the one that uses the mean daily temperature summing method (Laaidi, 2001; Laaidi et al., 2003; Garcia-Mozo et al., 2000; Majeed, 2018). This model, unlike others such as 'Growing Degrees Days', is not applied from the chilling stage, but from a statistically determined date (Garcia-Mozo et al., 2000). In Barcelona, winter chilling is usually interrupted by warmer events suppressing or decreasing the effects of the chilling temperatures (Chuine et al., 1999). The model that we adopted in the present work uses the summing temperatures method, which we chose since temperature is the best predicted variable by long-term climate models and also because of the simplicity of the model.

The emission scenarios, defined by the International Panel on Climate Change (IPCC, 2013), are a plausible representation of the future evolution of the emissions of substances that could be radiatively active. The first emission scenarios were presented in 1992 and were used to obtain the first climate projections. In the year 2000, the Special Report on Emissions Scenarios (SRES) (Nakicenovic and Swart, 2000), were adopted, which served as the basis for the climate projections presented in the Third and Fourth Assessment Reports of the IPCC (2001 and 2007, respectively). These scenarios considered a bundle of 'possible futures' for our societies, integrating a vast palette of evolutions determined by national economies, technological supply, energy choices, demography, changes in individual behaviour, etc. The SRES scenarios were organized into four well-known families: A1, A2, B1 and B2, which, translated into Greenhouse Gas (GHG) emissions, fed a chain of models to provide global climate evolution projections. However, these scenarios did not consider possible mitigation policies. In the Fifth Evaluation Report of the IPCC (AR5), a new set of four scenarios that do consider climate policies were used, the so-called Representative Concentration Pathways (RCP; IPCC, 2013). These RCPs were defined as scenarios that cover time series of emissions and concentrations of the

full range of GHGs and aerosols and chemically active gases, as well as land use and land cover (Moss et al., 2010; Amblar et al., 2017). RCPs are identified by the approximate total radiative forcing for the year 2100 with respect to 1750, which is considered to be in a range between 2.6 and 8.5 Wm^{-2}. In the case of RCP6.0 and RCP8.5, the radiative forcing does not reach its maximum until 2100 (approximately 670 and 936 ppm CO_2-e, respectively); for RCP2.6, it reaches a maximum (approximately 421 ppm CO_2-e) and then decreases; and for RCP4.5, it stabilizes around 2100 (approximately 538 ppm CO_2-e). More recently, socioeconomic factors were added to these scenarios in the so-called Shared Socioeconomic Pathways (Eyring et al., 2016; Riahi et al., 2017) to provide the description of different socio-economic developments, as defined in the IPCC Sixth Assessment Report (AR6) (IPCC, 2022).

Although the main driving mechanisms in plant phenology include temperature, photoperiod and winter cooling, in this work we have focused on the possible impact on the start date of the pollen season due to changes in temperature predicted by climate models. Our starting hypothesis is that the increase in temperatures expected for the end of the current century in the Mediterranean region, and specifically for the city of Barcelona, will have an important influence on the time in which pollination occurs. The objective of this work is to use a prediction model for the start date of pollen season coupled to the regionalized projected temperatures from different climate models in the most relevant scenarios described by the IPCC to obtain trends throughout the 21st century in the pollen season start dates of various taxa selected for their importance in the airborne pollen spectrum, most of them causing and triggering respiratory allergies: *Olea*, *Pinus*, *Pistacia*, *Plantago*, *Platanus*, and Deciduous *Quercus*.

2. Material and methods

2.1. Aerobiological data

Barcelona is a coastal city, located in the Catalan region, in the northeast of Spain. Catalonia is bordering with France by the Pyrenees in the north, with the Mediterranean Sea in the east and with the regions of Aragon and Valencia in the west and southwest. Complex terrain can be found along the Catalan coast due to littoral and pre-littoral mountain ranges and the corresponding planes and, in the north, due to the Pyrenees and pre-Pyrenees (Fig. 1). Barcelona lies in a plane, along the littoral range and the Mediterranean Sea, in the middle of the Catalan coast, 150 km far from the French border. Barcelona has a typically Mediterranean climate, characterized by mild temperatures and infrequent but sometimes torrential rains, concentrated mainly in autumn (Casas-Castillo et al., 2018; Llabrés-Brustenga et al., 2020). In the 20-year period studied here (2000–2019), the average annual rainfall in Barcelona was 620 mm, with an average annual temperature of 16 °C, and relative humidity of 68 %. The vegetation around the city of Barcelona is typically Mediterranean, with several species of the *Quercus* genus (the evergreen *Q. ilex* subsp. *ilex* and *Q. coccifera* and *Q. pubescens* as the main deciduous) and the corresponding cohort of species contributing to the main forests and *Pinus* (mainly *P. halepensis* and *P. pinea*) abundantly present. Inside the city, a long list of ornamental plants (*Platanus* the most abundant and *Olea* also frequently used) and ruderal species add their pollen to the airborne spectrum.

Airborne pollen data used in this study were obtained by the Aerobiological Network of Catalonia (Xarxa Aerobiològica de Catalunya, XAC) at Barcelona (41° 23′ 37.42" N, 2° 09′ 53.72″ E, 93 m a.s.l.) for the period 2000–2019. Daily samples were obtained from a Hirst sampler (Hirst, 1952), following the standardized method in European Aeroallergen Network (EAN) (Galán et al., 2014), and analysed following the standardized Spanish method (Spanish Aerobiology Network (REA) (Galán et al., 2007). Six pollen taxa important inside the city and in the surrounding landscape, most of them able to elucidate respiratory allergies and considered in previous studies by the authors (Izquierdo et al., 2011; Alarcón et al., 2023; Majeed et al., 2018; Rodríguez-Solà et al., 2022), were selected: *Olea*, *Pinus*, *Pistacia*, *Plantago*, *Platanus*, and Deciduous *Quercus* (D.*Quercus*). These taxa, accounting for 56 % of the airborne pollen spectrum in Barcelona, have a markedly seasonal start of flowering, with a year-to-year seasonal variability of, at most, five weeks.

The start of the pollen season (Observed Start Pollen Season, SPS_O) is defined here as the day in which the sum of the daily mean pollen concentrations reaches the 2.5 % of the annual sum (Andersen, 1991). The trend of the linear regression of the SPS_O for the period 2000–2019 was computed for the 6 pollen types. In order to compare SPS_O in the early and later years of the 20-year period and to smooth out interannual variations, we took initial (2000–2004) and final (2015–2019) periods and computed the differences between these two 5-year periods. Daily values of mean temperature covering the period 2000–2019, provided by the Servei Meteorològic de Catalunya (SMC) and recorded in the Fabra Observatory (41°25′N, 2°07′E, 415 m a.s.l.), at approximately 5 km north of the pollen sampling site, were used.

2.2. Forecasting method for the start date of the pollen season

The forecasting method used here consist of a model, the SDP prediction model, that predicts a statistical starting day of the pollen season (Forecasted Start Pollen Season, SPS_F) by cumulative summing of the daily mean temperatures from a set of trial dates and above a set of thermal thresholds. The first step consists of the determination of the

Fig. 1. Geographical location of the Barcelona aerobiological station in the Iberian Peninsula and Catalonia.

initial date for summing up temperatures, the temperature threshold, and the value of the cumulative sum to be reached for pollen season start. These initial parameters are calculated from the observed starting dates of each pollen type of the period 2000–2019. The set of initial dates are ranged from 1st January up to the SPS_O in steps of 10 days. The set of thermal thresholds tested are ranged from 0 °C to 9 °C in steps of 1 °C. For each combination of initial date and thermal threshold, the sum of the daily mean temperature above the thermal threshold from the initial date and until the SPS_O is calculated for each pollen type and year included in the forecasting method. The mean and the standard deviation (SD) of the sum of temperatures for all years is then computed for each combination. The best initial date and the more appropriate threshold are those that minimized the ratio SD/mean (coefficient of variation), providing also the corresponding cumulative sum of temperatures (Laaidi, 2001; Laaidi et al., 2003; Garcia-Mozo et al., 2000). We will call 'initial parameters' this set of three values. To facilitate the understanding, a detailed description of the calculations for *Platanus* is given in Section 3.3.

2.3. Climate models and scenarios

Regionalized projections from the global models participating in the Fifth Assessment Report (AR5) of the Intergovernmental Panel on Climate Change (IPCC) of future temperatures predicted for Barcelona were obtained from RESCCUE, a European project devised to analyse future urban impacts due to climate change (Monjo et al., 2020). RESCCUE Project collected and filtered temperature data through several tests (general consistency, outliers and inhomogeneities), in order to handle datasets long enough and of good quality, all available meteorological observations in the considered areas. As a way to obtain the best input possible, every valid station was extended in time by downscaling process with the ERA-Interim reanalysis (European Centre for Medium Weather Forecast, ECMWF). Future climate projections were obtained for ten global climate models from the Coupled Model Intercomparison Project (CMIP5). Although CMIP6, more recent, continues the evolution pattern of CMIP5 by adding Shared Socioeconomic Pathways (SSPs, Riahi et al., 2017), the comparison between both CMPIs carried out by Chen et al. (2020) obtained similar spatial patterns, and also similar high pattern correlations between the ensemble of multi-model medians of CMIP6 and CMIP5 and observations. Therefore, here we used the CMIP5 models for which RESCCUE makes regionalization available at the point of our interest, the Fabra Observatory in Barcelona. These models were downscaled through statistical methods (analogous stratification and transfer functions among others) to project local climate according to the identified climate drivers: temperature, precipitation, wind, relative humidity, sea level pressure, potential evapotranspiration, snowfall, wave height and sea level; and for both climate and decadal timescales. Already downscaled models were first validated for the method and afterwards verified, obtaining small errors and good coherent simulations.

The data set used in the present work consisted of daily forecast of the maximum and minimum temperature at the aforementioned Fabra Observatory station for the period 2006–2100 obtained from RESCCUE for five global climate models of the ten possible (BCC-CSM1.1, CNRM-CM5, MIROC-ESM-CHEM, MRI-CGCM3 and NorESM1) and the four main Representative Concentration Pathways (RCP) scenarios (RCP2.6, RCP4.5, RCP6.0 and RCP8.5) established in the IPCC (2013) report. We have chosen the models that RESCCUE provides with temperatures for at least 3 RCPs, with the exception of GFDL_ESM2M model. Scenarios and models used here are summarized in Table 1, as well as the bibliography with the physical description of the models.

In addition to the predicted temperatures for the 21st century in the different scenarios, all models provide the so-called 'historical control series' for the period 1951–2005, which can be used as a reference for the projected temperatures. The observed temperature data available in the Fabra Observatory series begin in 1995, and so the historical control period used in this study is 1995–2005.

Table 1
Information on the regionalized models used in the generation of the projected temperatures.

Model	Institution	Scenarios	References
BCC-CSM1.1	Beijing Climate Center, China	RCP2.6 RCP6.0 RCP8.5	Wu et al., 2013; Xiao-Ge et al., 2013
CNRM-CM5	Centre National de Recherches Météorologiques/Centre Européen de Recherche et Formation Avancée en Calcul Scientifique (CNRM-CERFACS), France	RCP2.6 RCP4.5 RCP8.5	Voldoire et al., 2013
MIROC-ESM-CHEM	AORI NIES JAMSTEC, Japan	RCP2.6 RCP4.5 RCP6.0 RCP8.5	Watanabe et al., 2011
MRI-CGCM3	Meteorological Research Institute, Japan	RCP2.6 RCP4.5 RCP6.0 RCP8.5	Yukimoto et al., 2012
NorESM1	Norwegian Climate Center (NCC), Norway	RCP2.6 RCP4.5 RCP6.0 RCP8.5	Bentsen et al., 2013

The non-parametric Spearman and Mann-Kendall rank correlation coefficients were calculated to measure the robustness of trends in the forecasted start dates (SPS_F). The significance of the obtained trends was evaluated by means of the Mann-Kendall test. Boxplots showing the median and the interquartile range (range between the 25th and 75th percentile) of the 5 models for the differences between the forecasted start days and the 'control start dates' for each scenario corresponding to the 38-year periods 2024–2061 and 2062–2100 for the 6 taxa at Barcelona were obtained.

2.4. Validation of the SDP prediction model

In order to measure the quality and the predictability power of the model, a double validation was carried out: an internal one in which the forecasted dates were evaluated against those observed for the years 2000–2019, and an external validation, statistically more limited, applying the model to obtain the start dates of the 4 years of the period 2020–2023, not included in obtaining the initial parameters.

The mean bias error (*MBE*) was used as a measure of the difference between forecasted and expected pollen season start dates:

$$MBE = \frac{1}{N}\sum_{i=1}^{N}\left(SPS_{Fi} - SPS_{Oi}\right)$$

The mean absolute error (*MAE*) and index of agreement (*IA*; Willmott, 1981) were used as measures of model error:

$$MAE = \frac{1}{N}\sum_{i=1}^{N}\left|SPS_{Fi} - SPS_{Oi}\right|$$

$$IA = 1.0 - \frac{\sum_{i=1}^{N}\left|SPS_{Oi} - SPS_{Fi}\right|^2}{\sum_{i=1}^{N}\left[\left|SPS_{Fi} - \overline{SPS_O}\right| + \left|SPS_{Oi} - \overline{SPS_O}\right|\right]^2}$$

where SPS_F and SPS_O are forecasted and observed values, and N is the total number of forecasted/observed pairs. Moreover, the root mean square error (*RMSE*) is a frequently used measure of the differences between the forecasted values predicted by a model and the values actually observed. Following Appel et al. (2007), the model performance was evaluated using systematic and unsystematic root mean square errors, $RMSE_s$ and $RMSE_u$, in order to identify the sources of error. The

$RMSE_s$ represents the portion of the error that is attributable to intrinsic error in the model (systematic) and the $RMSE_u$ represents random (unsystematic) errors in the model or model inputs that are less easily addressed:

$$RMSE_s = \sqrt{\frac{1}{N}\sum_{i=1}^{N}(SPS_i - SPS_{Oi})^2}$$

$$RMSE_u = \sqrt{\frac{1}{N}\sum_{i=1}^{N}(SPS_i - SPS_{Fi})^2}$$

$$SPS = a + b{\cdot}SPS_O$$

$$RMSE = \sqrt{(\mathrm{RMSE}_u)^2 + (\mathrm{RMSE}_s)^2}$$

a and b are the least-squares regression coefficients derived from the linear regression between SPS_F and SPS_O.

Therefore, the smaller the errors, the better the model and the ability to predict future values. For a good model behaviour, the unsystematic portion of the error ($RMSE_u$) must be much larger than the systematic portion, whereas a high $RMSE_s$ value indicates a poor model.

3. Results and discussion

3.1. Observed start dates

The average date of the 20-year period of the Observed Start Pollen Season, SPS_O, for the 6 pollen types under study are showed in Table 2. *Platanus* is the taxon that presents the least variability, around 24 days, while *Pinus* is the one having the greatest variability, around 40 days. *Pinus* is the earliest airborne pollen type, followed closely by *Platanus*. *Olea* pollen is the latest in becoming airborne.

In the 20-year period analysed here, the trends obtained from the slope of the SPS_O linear regression showed a delay for the start of pollen season in *Olea* (+1.20 day/decade), *Plantago* (+2.67 day/decade) and D. *Quercus* (+3.4 day/decade), and an advance in *Pinus* (−0.16 day/decade), *Pistacia* (−0.29 day/decade) and *Platanus*, (−1.12 day/decade), although all trends were non-significant (Table 2). These trends are lower, but of the same sign, than those found by Makra et al. (2011) in Szeged (Hungary) for the 11-year period 1999–2009: −7 days/decade in *Platanus*, −2 days/decade in *Pinus,* + 4 days/decade in D.*Quercus*, all non-significant. However, the differences are greater in *Plantago*, which showed, in Szeged, an advance of 23 days/decade at the significance level of 5 % (Mann-Kendall test).

To compare start dates in the early and later years, we took initial (2000–2004) and final (2015–2019) periods of 5 years, to smooth out interannual variations, and we computed the differences in the SPS_O between these two 5-year periods. We obtained a delay of 1 day for *Pistacia*, 2 days for *Olea* and *Pinus*, 3 days for *Plantago*, and 6 days for D. *Quercus* (Table 2). The pollen of *Platanus* was the only one presenting an advance, 2 days.

Table 2
Mean value of the observed dates (in day of the year) of the Start Pollen Season, SPS_O, for the six taxa recorded at the Barcelona station. Minimum (Min) and maximum (Max) dates during the period 2000–2019. Linear trend (days/decade). Average date in the earliest 5-year period 2000–2004; average date in the latest 5-year period 2015–2019. Difference between the earliest and the latest 5-year period (in number of days, positive corresponds to advance and negative to delay).

SPS_O	*Olea*	*Pinus*	*Pistacia*	*Plantago*	*Platanus*	*D.Quercus*
Mean	124	68	85	98	76	95
Min	106	46	73	81	67	78
Max	135	86	103	116	90	109
L. trend (non- sig.)	+1.20	−0.16	−0.29	+2.67	−1.12	+3.44
2000–2004	121	63	84	95	74	89
2015–2019	123	65	85	98	72	95
Difference	2	2	1	3	−2	6

A study carried out in the United Kingdom (UK) in the period 1995–2020 obtained significant trends in the advance of the start of the *Quercus* pollen season in 3 of 6 localities analysed (Adams-Groom et al., 2022). Another interesting study in the UK of the date of first flowering of more than 400 species of plants (trees, herbs and shrubs) distributed throughout the UK, found a global advance of 26 days between the periods 1753–1986 and 1987–2019 with a high level of significance ($p < 0.0001$) (Büntgen et al., 2022). The analysis of 751 time series in Central and Northern Europe corresponding to the period 1959–1996 on phenological trends in springtime phases such as leaf unfolding, needle flush and flowering, showed a mean linear trend of −2.1 day/decade (Menzel, 2000). However, another more recent study of Menzel et al. (2020) with observational data between 1951 and 2018 shows that these advances may show signs of reversibility. They found that the proportion of significant trends increased but the mean advances of the spring and summer phases decreased in the period after 2000, especially for fruit trees and wild plants, confirming the findings of Piao et al. (2019) of slowing or even reversing trends in recent years. he differences we found between our results and these others obtained in regions of Central and Northern Europe could be due to certain dependence on altitude that the study by Rojo et al. (2021) found. Barcelona is located at sea level and, according to this study, the higher the altitude, the greater the progress observed in flowering. Picornell et al. (2024) also not found significant trends in the start of *Platanus* for the period 1994–2022 in two Mediterranean localities in southern Spain.

3.2. Temperature projections from climate models for the 21st century

The projected temporal evolution of the daily mean temperature at the Fabra Observatory in Barcelona calculated by RESCCUE has been analysed for the months in which the conditions for pollination of the studied taxa occur: January, February, March, April and May. The linear adjustment obtained from the average daily temperatures predicted for the 5 months in the period 2024–2100 allowed us to estimate the variations *per* decade in this period, which are shown in Supplementary Materials Table S1 for each of the five models and the different scenarios considered in this study. All models and scenarios showed temperature increases for the 5 months (positive values), with the exception of January in MIROC-ESM RCP2.6 and April in MRI-CGCM3 RCP4.5. The Mann-Kendall test applied on the projected temperature series has shown that the positive trends found for the RCP8.5 scenarios are all significant (p-value $\leq$0.05, 25 out of 25), while 85 % (17 out of 20) are significant for the RCP6.0 scenarios. The percentage of significant cases decreases as the scenarios become less severe, so these trends were significant for 60 % of the RCP4.5 scenarios (12 out of 20) and only 28 % (7 out of 25) for RCP.2.6 scenarios. In total, there is a 68 % of significant positive trends.

The increase is quite important for the RCP6.0 and RCP8.5 scenario, 0.38 °C/decade and 0.50 °C/decade, respectively, on average considering the five models, and less pronounced for the other scenarios: 0.11 °C/decade (RCP2.6), 0.19 °C/decade (RCP4.5). MIROC-ESM and BCC-CSM1.1 are the models that present the most marked differences between scenarios, in February (0.79 °C/decade RCP8.5 and 0.05 °C/decade RCP2.6) for MIROC-ESM and May (0.87 °C/decade in RCP8.5 and 0,19 °C/decade in RCP2.6) for BCC-CSM1.1. In contrast, MRI-CGCM3 is the one that presents the smallest difference between scenarios, and this is for May.

Fig. 2 shows, as an example, the sequence from 2024 to the end of the 21st century of the monthly averages of daily mean temperature for the months from January to May for the MIROC-ESM model and the RCP8.5 scenario and the trend lines for the five months.

Here we analyse future trends in the months in which pollination

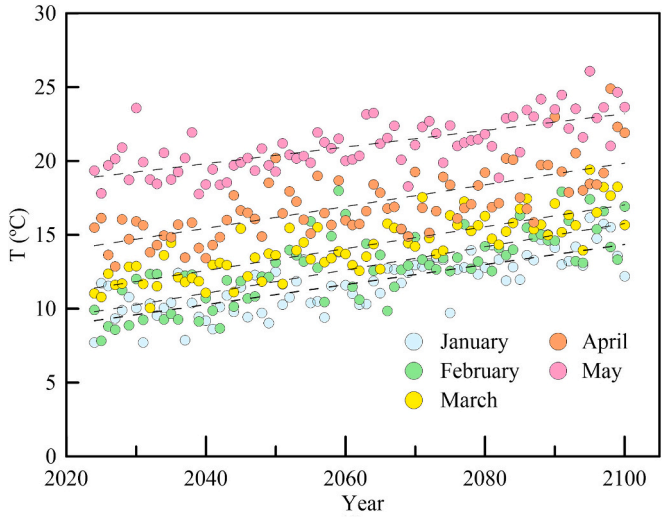

Fig. 2. Monthly average of the projected daily mean temperatures from the MIROC-ESM-CHEM model and RCP8.5 scenario for January, February, March, April and May 2024–2100 at the Fabra Observatory (Barcelona).

occurs, but we do not include the months in which pollen is fixed on tree flowers. However, a study carried out in the United Kingdom in the period 1995–2020, previously cited, obtained significant correlations ($p < 0.001$) between the start date of the *Quercus* pollen season and the maximum and minimum temperatures of the month of July of the previous year (Adams-Groom et al., 2022). Therefore, temperature changes in the summer months due to climate change may also affect the onset of spring pollen types.

3.3. Initial parameters of the SDP prediction model and model uncertainty

By computing the cumulative sum of temperatures from January 1st to the SPS_O (Table 3) for the years 2000–2019, the initial parameters needed as input data for the SDP prediction model, were obtained (initial date, temperature threshold and cumulated temperature). As shown in Table 3, *Olea* was the taxon with the highest sum of temperatures (1350 °C), while *Platanus* was the one that required a later beginning day (January 21) and, together with *Pistacia*, the highest temperature threshold (5 °C).

To facilitate the understanding of obtaining these initial parameters, we will describe in more detail the case of *Platanus*, in which 60 combinations were obtained (Table 4): 10 temperature thresholds by 6 initial dates (from January 1 to February 20). The mean and the standard deviation (SD) of the sum of temperatures for all years is then computed for each combination. The best initial date and the more appropriate threshold were those that minimized the ratio SD/mean (coefficient of variation), providing also the corresponding cumulative sum of temperatures. We will call 'initial parameters' this set of three values. In the example shown in Table 4 for *Platanus*, the best coefficient of variation was obtained for the initial date January 21, the thermal threshold of 5 °C, and the average sum of temperatures of 504.55 °C.

Table 3
Initial parameters obtained to forecast the Start of the Main Pollen Season (SPS_F) for each taxon.

Parameters	*Olea*	*Pinus*	*Pistacia*	*Plantago*	*Platanus*	D. *Quercus*
Initial date	1-Jan	1-Jan	11-Jan	1-Jan	21-Jan	1-Jan
Threshold (°C)	0	2	5	0	5	0
Sum of Temp (°C)	1350	607	708	972	505	935

These will be the initial parameters for this taxon from which the SDP prediction model will calculate the predicted start date for each year.

3.3.1. Internal validation

Using the obtained initial parameters of Table 3, the SPS_F were forecasted for the six taxa and the 20-year period 2000–2019. These predicted dates were then statistically compared with the observed ones SPS_O with the purpose of evaluating the quality of the SDP prediction model.

As an example of this comparison, in Table 5 are shown the observed and predicted dates for *Platanus*. In six of the years studied, the observed and predicted dates coincided. The predicted date advanced with respect to the observed one in ten of the years, by a maximum number of 4 days. In the remaining four years the observed date delayed, by a maximum number of 5 days. Fig. 3 shows the linear regression between observed and predicted dates for this same taxon and the high value obtained for the Pearson correlation coefficient ($R = 0.94$, at the significant level of p-value ≤ 0.005). As the graph shows, the slope of the relationship between the two variables is 0.96, which indicates a slight advance in the forecasted dates compared to those observed for *Platanus*.

The model uncertainty is shown in Table 6 for each taxon. For the six taxa the mean bias error (*MBE*) is negative, with absolute values oscillating between 0.4 and 0.6, meaning that the dates predicted by the SDP model, on average, advance half a day. The mean absolute error (*MAE*) was more diverse for the different taxa, being the highest for *Plantago* (4.9 days) and the lowest for *Platanus* (1.8 days).

The taxon with the least root mean square error (*RMSE,* 2.5 days) and the best agreement index (*IA,* 0.97) is *Platanus*, followed by *Pistacia* (3.3 days, 0.96); and the one with the biggest *RMSE* (7.5 days) and lowest *IA* (0.72) is D.*Quercus*. On the other hand, the systematic error ($RMSE_s$) was lower than the random error ($RMSE_u$) for all taxa, with the exception of *Pinus* (4.2 vs. 4.1), indicating a low intrinsic error (less than one day in the case of *Platanus*) and good performance of the model. The SDP model predicts quite accurately for pollen grains that have a marked seasonal character, with an interannual variability in the start date of a few weeks. Our results are similar to those found in Lyon (France) using the same model for the forecast of the start date of *Ambrosia* in which the differences between the predicted and observed date ranged between 0 and + 8 days (Laaidi et al., 2003). In several aerobiological stations located in Burgundy (Central France), the differences using the same method of summing temperatures, in this case for Poaceae, oscillated between −2 and + 4 days, depending on the location (Laaidi, 2001). The above-mentioned study by Picornell et al. (2024) in two Mediterranean locations in southern Spain in which a more complex model was applied considering the chilling phase prior to the temperature accumulation phase, obtained an *RMSE* of 4.4 days and a *MAE* of 3.2 days for *Platanus*, slightly higher values than those obtained by us.

3.3.2. External validation

The model was applied to the 4-year period 2020–2023, not included in the computation of the initial parameters. The observed and forecasted dates, as well as their difference and the mean bias error (*MBE*) are shown in Table 7. The *MBE* was greater than in the internal validation for most of the taxa, with the exception of *Pistacia*. The model advances the start of the pollen season between −1 and − 8.25 days in all taxa, except in *Pistacia*, which delays +0.5 days. Also, in the external validation, advances were obtained, in this case for all taxa, between −0.4 and − 0.6 days. Therefore, the validation results were better for the 20-year period than for this 4-year period. In the specific case of *Platanus*, in the 20-year period (Table 5), the difference between SPS_F and SPS_o ranged between - 4 and + 5 days, while in the 4-year period it ranged between −5 and 0 days. *D. Quercus* was the taxon with the highest *MBE* (−8.25). In the 20-year period *D. Quercus* is the one that gives the worst result for all the error measures analysed (Table 6). This result for *D. Quercus* does not seem to be related to the temporal variability it presents since in the period of 20 years it is 31 days (Table 2,

Table 4
Example of the obtention of the initial parameters (in italic and bold) for the SDP prediction model through the sum of temperatures, for *Platanus*. (SD: standard deviation).

Initial date		Sum of temperatures above a thermal threshold of									
01 JAN	year	0 °C	1 °C	2 °C	3 °C	4 °C	5 °C	6 °C	7 °C	8 °C	9 °C
	2000	681.45	681.45	679.65	679.65	675.95	675.95	653.95	616.15	601.55	490.45
	2001	698.40	698.40	698.40	698.40	698.40	693.50	688.20	662.05	624.75	532.40
	…	…	…	…	…	…	…	…	…	…	…
	2019	677.45	677.45	677.45	677.45	669.75	664.90	636.55	630.40	565.00	513.25
	Mean	696.59	696.44	695.33	692.89	687.23	677.15	653.77	620.41	557.18	481.29
	SD	45.10	45.29	45.40	46.91	47.43	47.83	55.66	64.62	86.31	93.86
	SD / Mean	0.06474	0.06503	0.06529	0.06770	0.06901	0.07063	0.08514	0.10416	0.15491	0.19502
11 JAN	year	0 °C	1 °C	2 °C	3 °C	4 °C	5 °C	6 °C	7 °C	8 °C	9 °C
	2000	591.80	591.80	590.00	590.00	586.30	586.30	564.30	526.50	519.10	442.20
	2001	594.15	594.15	594.15	594.15	594.15	589.25	583.95	564.45	534.75	450.40
	…	…	…	…	…	…	…	…	…	…	…
	2019	589.85	589.85	589.85	589.85	582.15	577.30	554.30	548.15	489.80	472.40
	Mean	605.66	605.57	604.52	602.43	597.13	587.99	566.77	537.59	484.41	425.40
	SD	35.60	35.61	35.44	35.68	34.84	34.18	42.48	51.40	71.58	74.62
	SD / Mean	0.05879	0.05881	0.05862	0.05923	0.05835	0.05813	0.07495	0.09561	0.14777	0.17541
21 JAN	year	0 °C	1 °C	2 °C	3 °C	4 °C	5 °C	6 °C	7 °C	8 °C	9 °C
	2000	521.40	521.40	519.60	519.60	515.90	515.90	499.80	493.80	493.80	442.20
	2001	504.00	504.00	504.00	504.00	504.00	499.10	493.80	480.90	466.30	415.50
	…	…	…	…	…	…	…	…	…	…	…
	2019	515.60	515.60	515.60	515.60	511.65	511.65	494.50	494.50	451.00	442.20
	Mean	520.04	519.95	518.89	517.20	512.99	***504.55***	486.72	464.93	425.30	380.97
	SD	31.40	31.40	31.15	31.64	30.22	***28.45***	35.83	43.79	61.44	65.13
	SD / Mean	0.06038	0.06039	0.06003	0.06117	0.05892	***0.05638***	0.07362	0.09419	0.14445	0.17095
…	…	…	…	…	…	…	…	…	…	…	…
20 FEB	year	0 °C	1 °C	2 °C	3 °C	4 °C	5 °C	6 °C	7 °C	8 °C	9 °C
	2000	222.70	222.70	222.70	222.70	222.70	222.70	222.70	222.70	222.70	205.20
	2001	185.60	185.60	185.60	185.60	185.60	180.70	175.40	162.50	147.90	147.90
	…	…	…	…	…	…	…	…	…	…	…
	2019	229.55	229.55	229.55	229.55	229.55	229.55	229.55	229.55	229.55	229.55
	Mean	258.61	258.59	258.34	257.65	256.06	253.11	248.18	242.27	227.95	215.64
	SD	59.33	59.31	59.11	58.65	58.10	57.40	57.43	58.47	56.45	56.94
	SD / Mean	0.22941	0.22936	0.22881	0.22765	0.22690	0.22679	0.23142	0.24135	0.24763	0.26405

difference between Max and Min), while for other taxa it is greater (*Pinus*, 40 days; *Plantago*, 35 days). In this internal validation we have not considered the other error measures since they do not have statistical significance as there is only a sample of 4 values.

Although temperature, which is the variable used in our model, is the first factor in controlling the onset of flowering as demonstrated by different studies (Ziska et al., 2019; Adams-Groom et al., 2022), the results of this study could be improved with 'process-based' models that also take into account other variables such as photoperiod and accumulated precipitation at the time of flowering. Using this type of models, Garcia-Mozo et al. (2009), in a study based on 12 years (1994–2005) of data at 12 stations in the Iberian Peninsula, obtained, in external validation over 2 years not included in the calibration, a root mean square error (RMSE) of about 4.5 days for the start date of Poaceae. This is a good result considering that the spatial variability in the start date over the stations studied is approximately 1 month and the temporal variability in a given station is about 1.5 months.

Our model does not consider the period of chilling temperatures, but it begins the temperature forcing at the beginning of quiescence. Chuine et al. (1999), in a study in two French stations, one located on the Mediterranean coast and another inland, obtained, from examining different assumptions of budburst models with 12 species, that it was better to consider forcing temperatures active from the onset of quiescence and not from the onset of dormancy. The same study showed that the models that included chilling temperatures were appropriate for the inland locality, but not for the coastal one, as is the case of Barcelona, in which the effect of winter chilling is frequently interrupted by warm episodes.

3.4. Application of the SDP prediction model to the projected temperatures

For each of the six taxa, the future start dates of pollen season SPS_F for each year in the period 2006–2100 were obtained, based on the temperature projections of the five climate models and the different scenarios, by using the SDP prediction model. Once the forecasted dates were obtained, in order to summarize the strength and direction of the trends throughout the 21st century and their level of significance, the Spearman and Mann-Kendall correlation coefficients were computed. Table 8 shows these coefficients for the significant trends (p-value ≤ 0.05 and p-value ≤ 0.05).

All models presented negative trends for the six taxa, which means that they predicted a progressive advance in flowering throughout the 21st century. A total of 86 % of the trends were significant. The only scenario that did not show significant trends for any taxon was RCP2.6 for the BCC-CSM1.1 and CNRM-CM5 models. However, MRI-CGM3 and NorESM1 did present significant trends in this scenario for all taxa, and MIROC-ESM only for *Olea*, *Pinus* and *Plantago*, these last two at the lowest significance level ($p \leq 0.05$).

In order to compare future flowering dates with past flowering dates, the SDP prediction model was applied to the 'historical control series' of temperature provided with each RESCCUE climate model, thus obtaining the 'control start dates' for the period 1995–2005. The evolution throughout the 21st century of the start day computed for the different scenarios for *Platanus* according to the MIROC-ESM model, *Olea* according to the NorESM1 model, and *Pistacia* according to the MRI-CGM3 model, are shown in Figs. 4, 5 and 6, respectively, as examples. The projected start dates correspond to the green, yellow, orange and red dots, depending on the RCP scenario, for the period 2006–2100. The grey dots correspond to the 'control start dates' (1995–2005) and the overlapping blue ones correspond to the start day observed from the

Table 5
Observed Start Pollen Season SPS_O, Predicted Start Pollen Season SPS_F, and start pollen season obtained by linear regression *SPS*, and their differences for *Platanus*.

Platanus	SPS_O	SPS_F	SPS	$SPS_F - SPS_O$	$SPS - SPS_O$	$SPS - SPS_F$
2000	10/3/2000	9/3/2000	9/3/2000	−1	−0.2	0.8
2001	9/3/2001	9/3/2001	8/3/2001	0	−0.1	−0.1
2002	11/3/2002	7/3/2002	10/3/2002	−4	−0.2	3.8
2003	21/3/2003	17/3/2003	20/3/2003	−4	−0.6	3.4
2004	21/3/2004	20/3/2004	20/3/2004	−1	−0.6	0.4
2005	31/3/2005	30/3/2005	29/3/2005	−1	−0.9	0.1
2006	22/3/2006	22/3/2006	21/3/2006	0	−0.6	−0.6
2007	11/3/2007	8/3/2007	10/3/2007	−3	−0.2	2.8
2008	7/3/2008	11/3/2008	6/3/2008	4	−0.1	−4.1
2009	15/3/2009	17/3/2009	14/3/2009	2	−0.3	−2.3
2010	26/3/2010	29/3/2010	24/3/2010	3	−0.7	−3.7
2011	21/3/2011	21/3/2011	20/3/2011	0	−0.6	−0.6
2012	23/3/2012	19/3/2012	22/3/2012	−4	−0.7	3.3
2013	22/3/2013	22/3/2013	21/3/2013	0	−0.6	−0.6
2014	15/3/2014	13/3/2014	14/3/2014	−2	−0.3	1.7
2015	22/3/2015	21/3/2015	21/3/2015	−1	−0.6	0.4
2016	7/3/2016	7/3/2016	6/3/2016	0	−0.1	−0.1
2017	10/3/2017	10/3/2017	9/3/2017	0	−0.2	−0.2
2018	15/3/2018	20/3/2018	14/3/2018	5	−0.3	−5.3
2019	9/3/2019	8/3/2019	8/3/2019	−1	−0.1	0.9

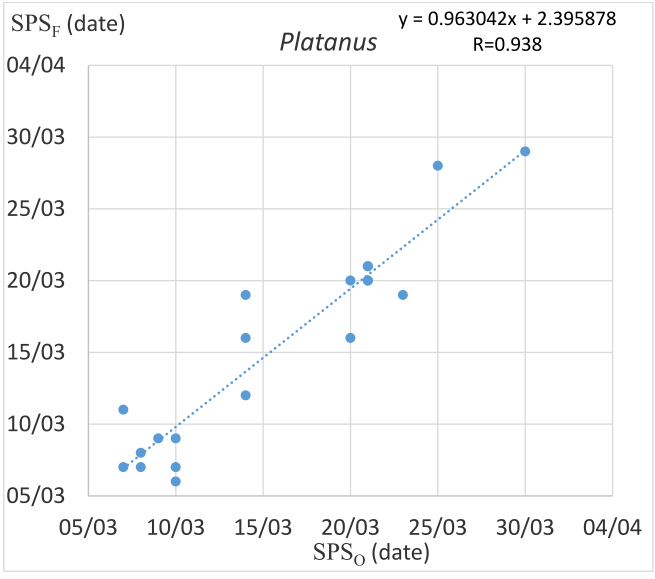

Fig. 3. Linear regression between Observed Start Pollen Season SPS_O and Predicted Start Pollen Season SPS_F for *Platanus*.

Table 6
Measures of the model uncertainty for each taxon, expressed in number of days, with the exception of *IA* which is a dimensionless parameter.

	Olea	*Pinus*	*Pistacia*	*Plantago*	*Platanus*	D.*Quercus*
MBE	−0.5	−0.5	−0.5	−0.6	−0.4	−0.4
MAE	4.4	4.7	2.8	4.9	1.8	6.1
IA	0.77	0.87	0.96	0.84	0.97	0.72
RMSE	6.1	5.8	3.3	6.0	2.5	7.5
$RMSE_s$	3.2	4.2	1.5	3.3	0.5	4.2
$RMSE_u$	5.2	4.1	3.0	5.0	2.4	6.2

Table 7
External validation: observed and forecasted dates of the pollen season for the years 2020–2023 and mean bias error (*MBE*) of the SDP model for the six taxa.

		2020	2021	2022	2023	*MBE*
Olea	SPS_O	28/4	30/4	7/5	23/4	−1.8
	SPS_F	24/4	4/5	29/4	24/4	
	$SPS_F - SPS_O$	−4	4	−8	1	
Pinus	SPS_O	19/2	8/3	23/2	13/3	−1.0
	SPS_F	24/2	5/3	25/2	5/3	
	$SPS_F - SPS_O$	5	−3	2	−8	
Pistacia	SPS_O	10/3	15/3	15/3	27/3	0.5
	SPS_F	12/3	18/3	18/3	21/3	
	$SPS_F - SPS_O$	2	3	3	−6	
Plantago	SPS_O	6/4	7/4	6/4	30/3	−4.8
	SPS_F	26/3	4/4	1/4	30/3	
	$SPS_F - SPS_O$	−11	−3	−5	0	
Platanus	SPS_O	2/3	9/3	11/3	18/3	3.0
	SPS_F	2/3	6/3	7/3	13/3	
	$SPS_F - SPS_O$	0	−3	−4	−5	
D.*Quercus*	SPS_O	5/4	1/4	13/4	31/3	−8.3
	SPS_F	22/3	1/4	29/3	27/3	
	$SPS_F - SPS_O$	−14	0	−15	−4	

actual pollen data in the period 2000–2019 (SPS_O). The observed values (blue) are indicated only as additional information, the comparison between projected and historical must be made with the 'historical control series' (grey). In the case of *Platanus*, the figure shows that there is a small negative trend, but it is non-significant, for the RCP2.6 scenario, in agreement with Table 8. However, for this same scenario, the slope of the linear regression is greater in the *Olea* and *Pistacia* graphs, consistent with the obtained significant negative trends (Table 8). In the three taxa, a sustained trend towards a progressive advance of pollen seasons in the most polluting scenarios is observed. For *Platanus* and *Olea,* smaller interannual oscillations are also observed in the least polluting scenarios that are not appreciated in *Pistacia*. In general, the correlation coefficients are higher for the higher emissions scenarios (Table 8).

Fig. 7 shows the advancement in number of days at the end of the 77-year period (2024–2100) with respect to the first year of the period according to the four scenarios for the five models and six taxa. The only model that gives a delay in flowering, although of a few days, is the CNRM-CM5 model for the RCP2.6 scenario and for all taxa except *Pistacia*. For the RCP8.5 scenario, the MIROC-ESM model is the one that predicts the greatest advances in pollen season start dates, between 19 and 34 days, depending on the taxon. On the other hand, *Olea* is the taxon that advances pollination the most, between 20 days (according to BCC-CSM1.1 and CNRM-CM5) and 34 days (MIROC-ESM). In the case of *Pinus*, this result in which MIROC-ESM projects a greater advance than the other models (22 days), is coherent since *Pinus* is the taxon that presents the earliest observed flowering dates (Feb 15 - Mar 27, Table 2), and MIROC-ESM is the model with the highest temperature increase *per* decade for the month of February (0.86 °C/decade, Table S1). For *Pistacia*, *Platanus*, *Plantago* and D.*Quercus*, although they flower a little later, March/April, also for these months MIROC-ESM is the one that gives a greater temperature increase *per* decade (0.81 °C/decade, Table S1).

Table 8
Mann-Kendall (τ) and Spearman (ρ) correlation coefficients of the significant trends ($p \leq 0.01$) obtained for the forecasted start dates (SPS_F) for all taxa and the different models and scenarios in the period 2006–2100 at Barcelona. Values in bold correspond to $p \leq 0.05$.

	Olea		*Pinus*		*Pistacia*		*Plantago*		*Platanus*		*D. Quercus*	
	τ	ρ	τ	ρ	τ	ρ	τ	ρ	τ	ρ	τ	ρ
BC_CSM1												
RCP26												
RCP60	−0.47	−0.65	−0.38	−0.54	−0.41	−0.58	−0.45	−0.62	−0.35	−0.5	−0.44	−0.61
RCP85	−0.51	−0.69	−0.38	−0.53	−0.41	−0.56	−0.47	−0.64	−0.33	−0.45	−0.47	−0.64
CMRM_CM5												
RCP26												
RCP45	−0.28	−0.39	−0.21	−0.31	−0.2	−0.29	−0.23	−0.33	**−0.16**	**−0.24**	−0.23	−0.33
RCP85	−0.58	−0.77	−0.54	−0.73	−0.54	−0.73	−0.55	−0.75	−0.5	−0.68	−0.55	−0.74
MIROC_ESM												
RCP26	−0.21	−0.31	**−0.15**	**−0.24**			**−0.15**	**−0.22**				
RCP45	−0.54	−0.73	−0.34	−0.55	−0.46	−0.63	−0.51	−0.64	−0.39	−0.55	−0.51	−0.69
RCP60	−0.71	−0.88	−0.56	−0.75	−0.58	−0.78	−0.63	−0.83	−0.53	−0.71	−0.62	−0.82
RCP85	−0.73	−0.9	−0.68	−0.86	−0.66	−0.84	−0.7	−0.88	−0.63	−0.82	−0.69	−0.87
MRI_CGM3												
RCP26	−0.22	−0.32	−0.19	−0.29	−0.24	−0.36	−0.24	−0.36	**−0.18**	−0.27	−0.24	−0.35
RCP45	−0.34	−0.48	−0.34	−0.49	−0.34	−0.47	−0.39	−0.54	−0.31	−0.44	−0.39	−0.54
RCP60	−0.46	−0.63	−0.35	−0.49	−0.37	−0.52	−0.41	−0.57	−0.35	−0.5	−0.42	−0.57
RCP85	−0.58	−0.77	−0.54	−0.73	−0.53	−0.72	−0.57	−0.76	−0.49	−0.67	−0.57	−0.76
NorESM1												
RCP26	−0.31	−0.44	−0.22	−0.31	−0.22	−0.31	−0.29	−0.41	**−0.16**	**−0.23**	−0.27	−0.39
RCP45	−0.41	−0.59	−0.32	−0.47	−0.32	−0.48	−0.38	−0.55	−0.29	−0.44	−0.37	−0.55
RCP60	−0.48	−0.66	−0.5	−0.69	−0.42	−0.58	−0.45	−0.61	−0.39	−0.55	−0.46	−0.62
RCP85	−0.53	−0.73	−0.44	−0.62	−0.42	−0.6	−0.49	−0.67	−0.41	−0.57	−0.48	−0.66

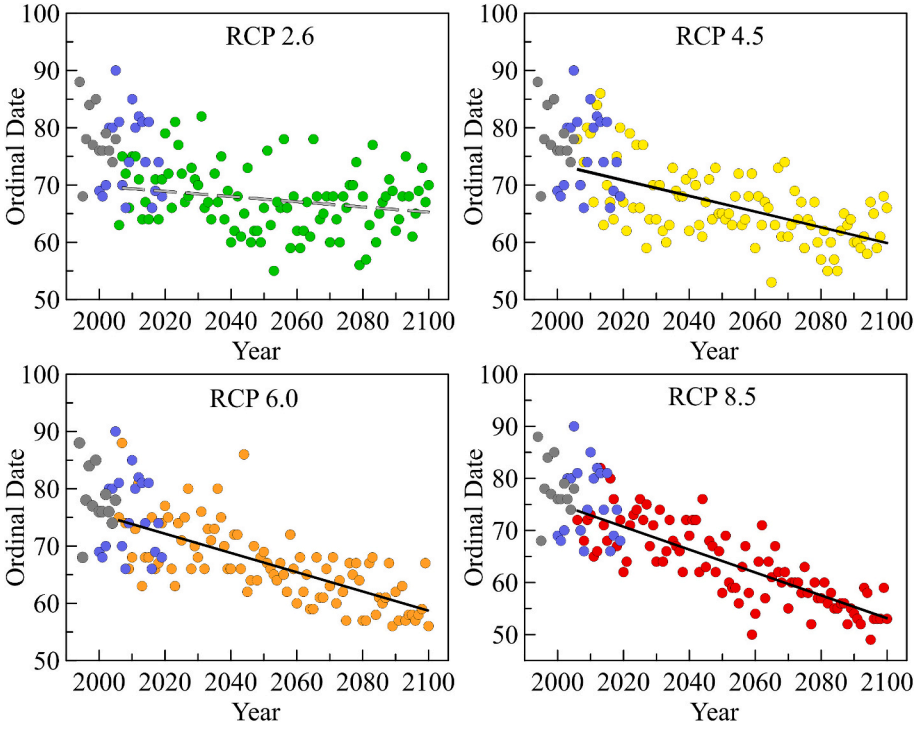

Fig. 4. MIROC-ESM model projected start dates (in day of the year) for *Platanus* for the period 2006–2100 at Barcelona. Grey: 'control start dates' (1995–2005). Blue: observed start dates (2000–2019). Black lines: significant linear fit; grey lines: non-significant linear fit (*p*-value ≤0.05).

Considering the set of results of the five models, we computed the differences between the forecasted start days in future years (2024–2100) and the 'control start dates' obtained from the 'historical control series' (1995–2005). Fig. 8 shows the boxplots with the values of the five models showing the median and the interquartile range (range between the 25th and 75th percentile) of the differences between the forecasted start days and the 'control start dates' for each scenario corresponding to the 38-year period 2024–2061 for the 6 taxa. In this

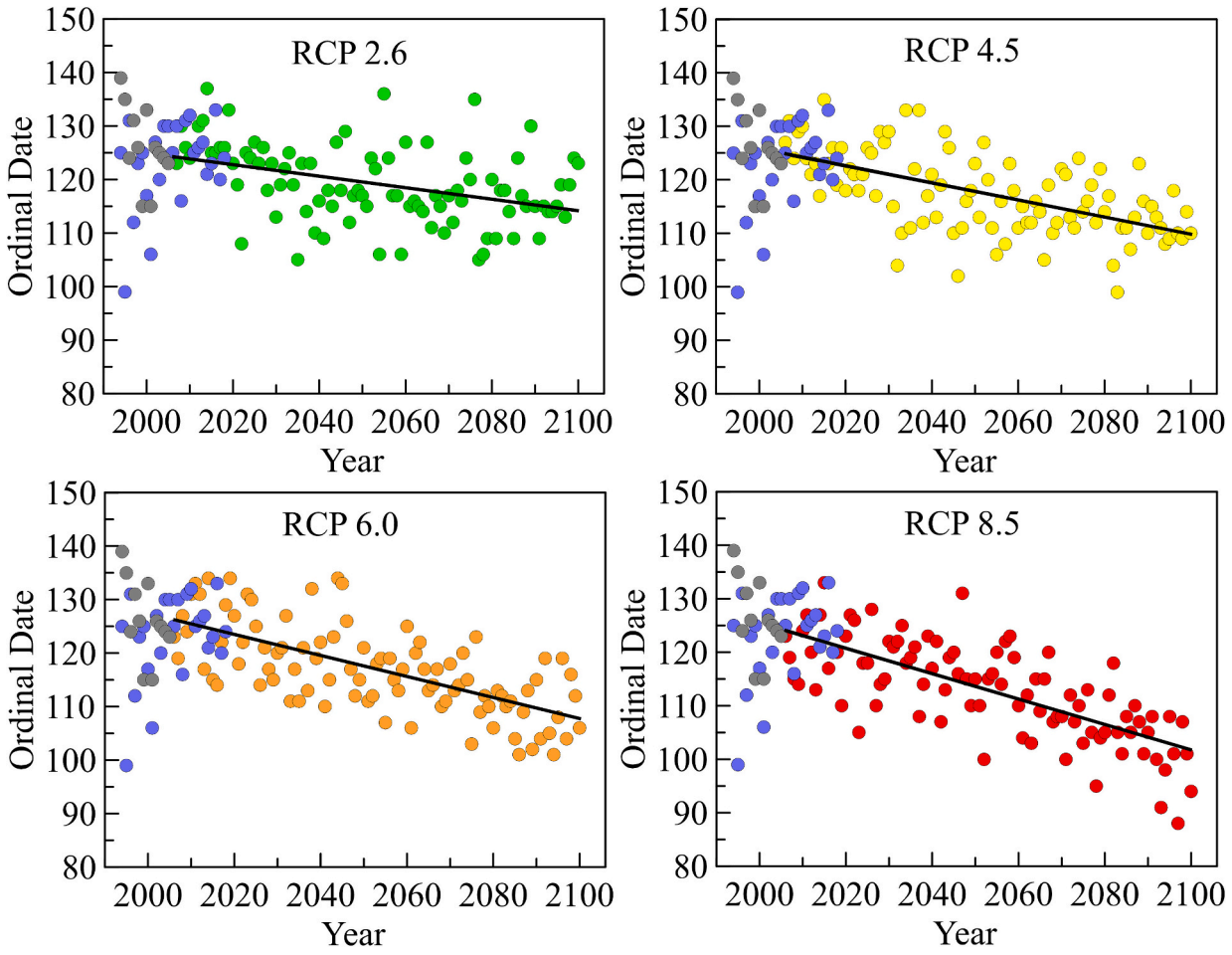

Fig. 5. NorESM1 model projected start dates (in day of the year) for *Olea* for the period 2006–2100 at Barcelona. Grey: 'control start dates' (1995–2005). Blue: observed start dates (2000–2019). Black lines: significant linear fit; grey lines: non-significant linear fit (p-value $\leq$0.05).

initial period, a marked advance in the start dates is already obtained with respect to the historical control period of between 5 and 10 days, depending on the scenario and the taxon. However, for *Olea*, the three scenarios RCP4.5, RCP6.0 and RCP8.5, give similar advancements. For *Pistacia*, *Plantago* and D.*Quercus*, the highest median values correspond to RCP4.5 scenario. The differences between scenarios are much more pronounced if calculated for the second half of the period (years 2062–2100). The two emissions stabilization scenarios (RCP4.5 and RCP60) show similar values, although slightly lower in the scenario in which stabilization occurs earlier (RCP4.0). The differences are very large between the RCP2.6 and RCP8.5 scenarios for all taxa, especially for *Olea*.

As far as we know, the present study obtains for the first time future projections throughout the entire 21st century of the start of the pollen season for a set of pollen types. Other recent works have focused on the influence of climate change on the dynamics of airborne pollen or on the phenology of plants by studying correlations between the changes experienced by the most influential meteorological variables and long-term pollen data (Bruffaerts et al., 2018; De Weger et al., 2021; Gehrig and Clot, 2021; Adams-Groom et al., 2022; Büntgen et al., 2022). Anderegg et al. (2021) found widespread advances and lengthening of pollen seasons, as well as increases in concentrations in North America, strongly related to the observed warming. The study attributed approximately 50 % of the seasonal trend in pollen and approximately 8 % of the trend in pollen concentrations to anthropogenic climate change. In the recent work of Picornell et al. (2024), the PhenoFlex statistical framework was used to project the phenology of *Platanus* in the period 2023–2050 based on the SSP1_2.6, SSP2_4.5 and SSP 5_8.5 scenarios from the CMPI6, at two Spanish localities. They do not find significant trends in the future start in one of the locations (Badajoz), while in the other one (Málaga) they found a slight delay attributed to a delay on the date of chilling requirement.

3.5. Limitations of the model

Models are a useful tool to understand the mechanisms that govern natural processes, represent them and make predictions. Accuracy and simplicity are the two attributes that are sought in a model, or a balance between both. The purpose of this work is not to model the complete phenological cycle of the studied plants, but to predict the moment in which their pollen appears in the air. This has allowed us to simplify the multiple environmental factors that govern phenology. The prediction model used here is based on the dependence of the start of the pollen season on the daily mean air temperature in the months prior to flowering. A possible limitation of the model when applying it to future projections may appear if the temperature range is outside the range of historical temperatures, since the linear relationship applied by the model may not be correct outside of the known conditions. Another limitation may be due to the fact that the future projections of the different scenarios only include meteorological variables. Changes in land use, such as reforestation, introduction or elimination of ornamental plants, decrease or replacement of autochthonous species, agricultural uses, can result in changes in the annual pollen integral. Since our model calculates the start date from a percentage of the annual pollen integral, these possible future changes introduce uncertainty into our model projections. Other sources of uncertainty are future changes

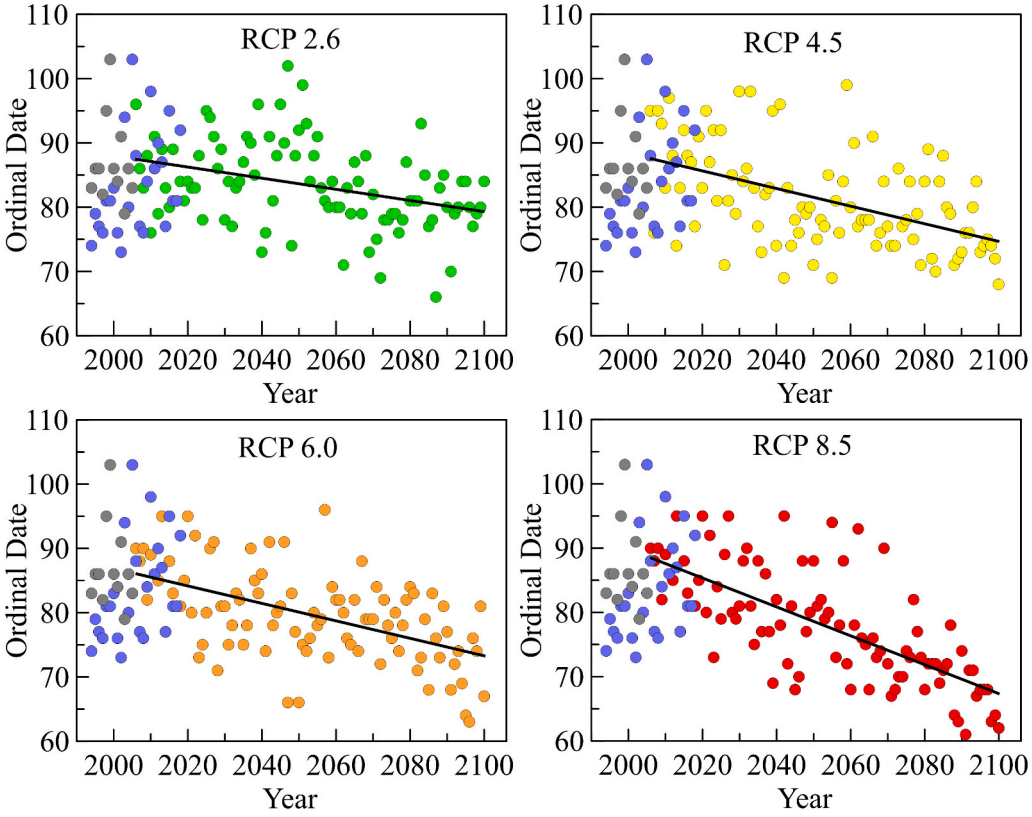

Fig. 6. MRI-CGM3 model projected start dates (in day of the year) for *Pistacia* for the period 2006–2100 at Barcelona. Grey: 'control start dates' (1995–2005). Blue: observed start dates (2000–2019). Black lines: significant linear fit; grey lines: non-significant linear fit (p-value $\leq$0.05).

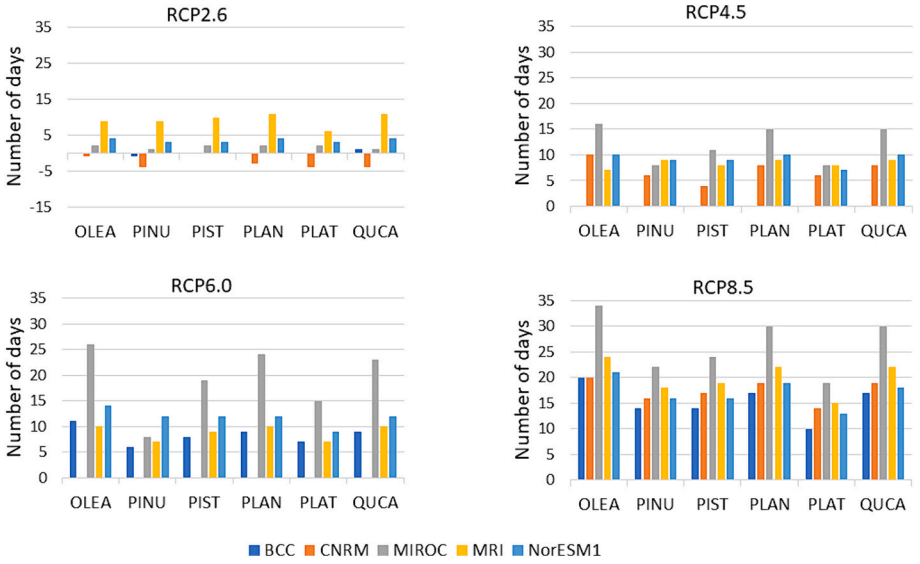

Fig. 7. Number of days in which flowering is advanced at the end of the period (year 2100) with respect to the beginning (year 2024) at Barcelona for *Olea* (OLEA), *Pinus* (PINU), *Pistacia* (PIST), *Plantago* (PLAN), *Platanus* (PLAT) and *D. Quercus* (QUCA).

in synoptic meteorology and atmospheric transport patterns, which may affect the pollen parameters of those species of regional or distant origin. Other factors to take into account are the delay in flowering that plants may experience as a result of a delay in the dormancy phase caused by increased temperatures and which would counteract the advances obtained by our model.

4. Summary and conclusions

In this work we have verified the starting hypothesis that an advancement in flowering is expected throughout the 21st century for different pollen types abundant in the city of Barcelona, most of them susceptible to causing respiratory allergies. Focusing on 20 years of observed flowering start dates (2000–2019), we have obtained an already existing advance for *Pinus*, *Pistacia* and *Platanus*. However, *Olea*,

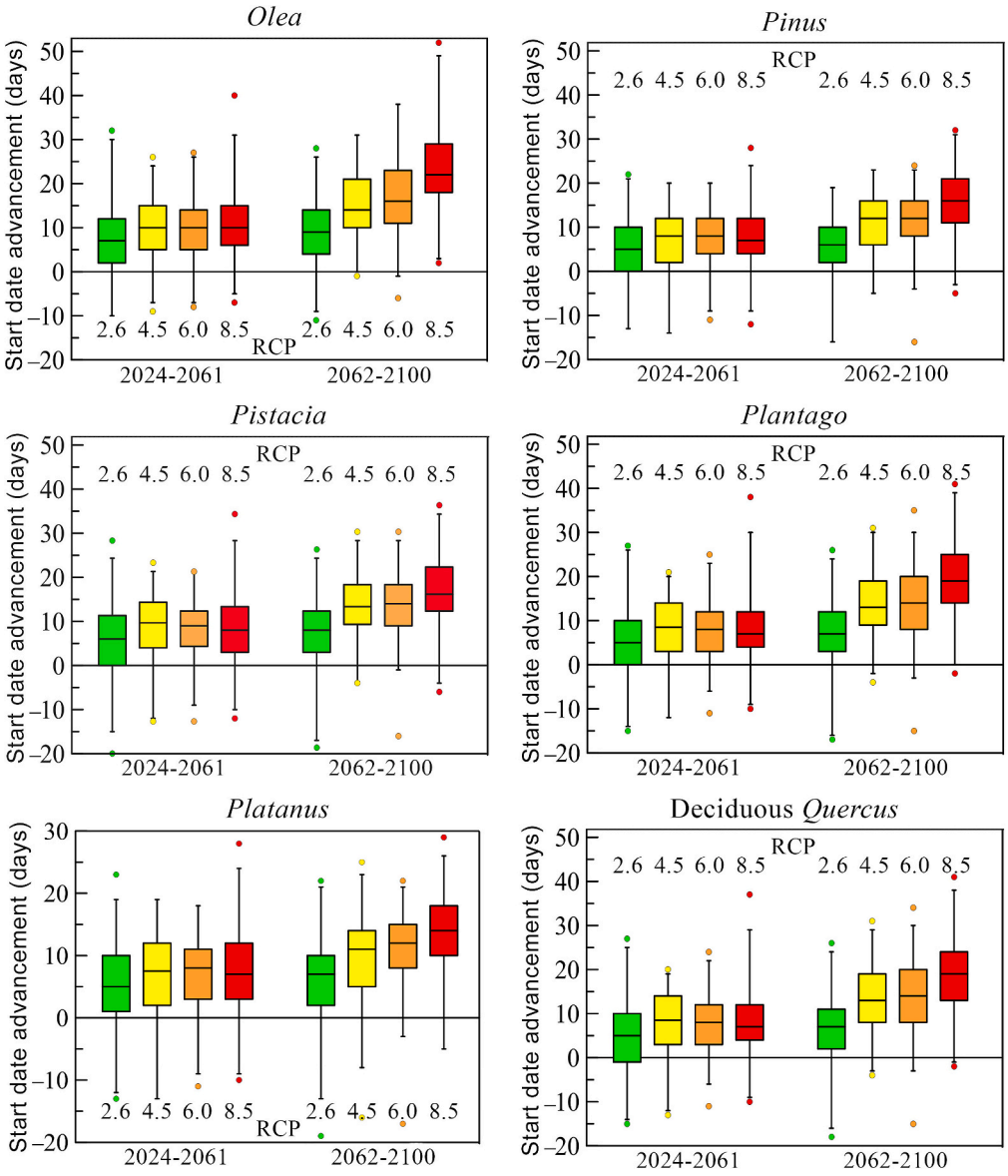

Fig. 8. Boxplots showing the median and the interquartile range (range between the 25th and 75th percentile) of the 5 models for the differences between the forecasted start dates and the 'control start dates' for each scenario corresponding to the 38-year periods 2024–2061 and 2062–2100 for the 6 taxa at Barcelona.

Plantago and D.*Quercus* show delay in this period. We have applied a statistical forecast model, the SDP prediction model, to the projected temperatures of five global climate models regionalized to the city of Barcelona, for the 4 scenarios proposed by the IPCC, with the purpose of predicting the future flowering dates. The SDP prediction model applied to the period 2006–2100 showed negative trends for the six taxa, indicating an advancement in the dates of the start of pollen season, 86 % of the obtained trends were significant. Thus, all climatic models resulted in earlier flowering, and this advance in the start of the pollen season was more marked in the most pessimistic scenarios. Only the mildest of the scenarios, RCP2.6, did not give significant trends for two of the models. In the most emissive scenario, RCP8.5, advances in flowering at the end of the century ranged, on average for the six pollen types, between 15 days (BCC-CSM1.1) and 27 days (MIROC-ESM), while for the stabilization scenario, RCP4.5, the advances ranged between 7 days (CNRM-CM5) and 12 days (MIROC-ESM). These results are consistent with the evolution of the projected daily mean temperature values. At the end of the 21st century, the increase in temperature predicted by climate models for the months in which the flowering occurs for the studied taxa is very important in the RCP8.5 scenario, ranging between 4 °C (May) and 6 °C (February and April) on average considering the five models. All taxa were sensitive to these increases in temperature, the most being *Olea*, and the least *Platanus*. Although the systematic error of the SDP prediction model is an advancement of 2.8 days on average for the six taxa, this is small and does not explain the high values in the number of days that we obtain at the end of this century, which can therefore be attributed to global warming. These results are preliminary but nevertheless indicate a trend. In the future, pollen season predictions can be improved using more complex models to obtain the full phenological response of plants to warming, based, for example, on machine learning techniques. However, it must be considered that changes in ornamental uses or agriculture, the delay or lack of chilling, as well as the possible adaptation of species to climate change, may delay or reverse the predicted changes.

Supplementary data to this article can be found online at https://doi.org/10.1016/j.scitotenv.2024.173363.

CRediT authorship contribution statement

Marta Alarcón: Writing – review & editing, Writing – original draft,

Software, Methodology, Conceptualization. **María del Carmen Casas-Castillo:** Writing – review & editing, Methodology, Investigation, Data curation, Conceptualization. **Raül Rodríguez-Solà:** Writing – review & editing, Methodology, Data curation, Conceptualization. **Cristina Periago:** Writing – review & editing, Methodology, Data curation, Conceptualization. **Jordina Belmonte:** Writing – review & editing, Methodology, Data curation, Conceptualization.

Declaration of competing interest

The authors declare that they have no known competing financial interests or personal relationships that could have appeared to influence the work reported in this paper.

Data availability

The authors do not have permission to share data.

Acknowledgements

We acknowledge the financial support of the European Commission for ENV4-CT98-0755; the Spanish Government for AMB97-0457-CO7-021, REN2001-10659-CO3-01, CGL2004-21166-E, CGL2005-07543/CLI, CGL2009-11205, CGL2012-39523-C02-01/CLI, CGL2012-39523-C02-01, CGL2012-39523-C02-02, CGL2016-75996-R, CTM2017-89565-C2-1-P, CTM2017-89565-C2-2, grant PID2020-117873RB-I00 funded by MCIN/AEI/10.13039/501100011033 and CONSOLIDER GRACCIE; the Catalan Government agency AGAUR for 2002SGR00059, 2005SGR00519, 2009SGR1102, and 2014SGR1274; Sociedad Española de Alergología e Inmunología Clínica (SEAIC); Laboratorios LETI PHARMA; Societat Catalana d'Al·lèrgia i Immunologia Clínica (SCAIC); Stallergenes Ibérica; S.A.; J Uriach y Compañia; S.A. This research contributes to the "María de Maeztu" Programme for Units of Excellence of the Spanish Ministry of Science and Innovation (CEX2019-000940-M). The authors gratefully acknowledge the Servei Meteorològic de Catalunya and RESCCUE Project for the data used in this publication.

References

Adamov, S., Pauling, A., 2023. A real-time calibration method for the numerical pollen forecast model COSMO-ART. Aerobiologia 39, 327–344. https://doi.org/10.1007/s10453-023-09796-5.

Adams-Groom, B., Selby, K., Derrett, S., Frisk, C.A., Pashley, C.H., Satchwell, J., King, D., Mckenzie, G., Neilson, R., 2022. Pollen season trends as markers of climate change impact: *Betula*. Quercus and Poaceae. Sci. Total Environ. 831, 154882 https://doi.org/10.1016/j.scitotenv.2022.154882.

Ahlholm, J.U., Helander, M.L., Savolainen, J., 1998. Genetic and environmental factors affecting the allergenicity of birch (*Betula pubescens* ssp. czerepanovii [Orl.] Hämet-ahti) pollen. Clin. Exp. Allergy 1998 Nov;28 (11), 1384–1388. https://doi.org/10.1046/j.1365-2222.1998.00404.x. PMID: 9824411.

Alarcón, M., Periago, C., Pino, D., Mazón, J., Casas-Castillo, M.C., Ho-Zhang, J.J., De Linares, C., Rodríguez-Solà, R., Belmonte, J., 2022. Potential contribution of distant sources to airborne *Betula* pollen levels in northeastern Iberian Peninsula. Sci. Total Environ. 818 https://doi.org/10.1016/j.scitotenv.2021.151827.

Alarcón, M., Rodríguez-Solà, R., Casas-Castillo, M.C., Molero, F., Salvador, P., Periago, C., Belmonte, J., 2023. Influence of synoptic meteorology on airborne allergenic pollen and spores in an urban environment in northeastern Iberian Peninsula. Sci. Total Environ. 896, 16533. https://doi.org/10.1016/j.scitotenv.2023.165337.

Amblar, P., Casado, M.J., Pastor, A., Ramos, P., Rodríguez, E., 2017. Guía de escenarios regionalizados de cambio climático sobre España a partir de los resultados del IPCC-AR5. In: Ministerio de agricultura y pesca, alimentación y medio ambiente, Agencia Estatal de Meteorología, Madrid, Spain, p. 96. https://www.aemet.es/es/conocermas/recursos_en_linea/publicaciones_y_estudios/publicaciones/detalles/Guia_escenarios_AR5.

Anderegg, W.R., Abatzoglou, J.T., Anderegg, L.D., Bielory, L., Kinney, P.L., Ziska, L., 2021. Anthropogenic climate change is worsening north American pollen seasons. Proc. Natl. Acad. Sci. 118 (7), e2013284118 https://doi.org/10.1073/pnas.2013284118.

Andersen, T.B., 1991. A model to predict the beginning of the pollen season. Grana 30 (1), 269–275. https://doi.org/10.1080/00173139109427810.

Appel, K.W., Gilliland, A.B., Sarwar, G., Gilliam, R.C., 2007. Evaluation of the community multiscale air quality (CMAQ) model version 4.5: sensitivities impacting model performance: part I-ozone. Atmos. Environ. 41 (40), 9603–9615. https://doi.org/10.1016/j.atmosenv.2007.08.044.

Ariano, R., Giorgio, Walter, Canonica, G.W., Passalacqua, G., 2010. Possible role of climate changes in variations in pollen seasons and allergic sensitizations during 27 years. Ann. Allergy Asthma Immunol. 104, 215–222. https://doi.org/10.1016/j.anai.2009.12.005.

Bayr, D., Plaza, M.P., Gilles, S., Kolek, F., Leier-Wirtz, V., Traidl-Hoffmann, C., Damialis, A., 2023. Pollen long-distance transport associated with symptoms in pollen allergics on the German Alps: An old story with a new ending? Sci. Total Environ. Jul 10;881, 163310. https://doi.org/10.1016/j.scitotenv.2023.163310.

Bentsen, M., Bethke, I., Debernard, J.B., Iversen, T., Kirkevåg, A., Seland, Ø., Drange, H., Roelandt, C., Seierstad, I.A., Hoose, C., Kristjánsson, J.E., 2013. The Norwegian earth system model, NorESM1-M – part 1: description and basic evaluation of the physical climate. Geosci. Model Dev. 6, 687–720. https://doi.org/10.5194/gmd-6-687-2013.

Bogawski, P., Borycka, K., Grewling, Ł., Kasprzyk, I., 2019. Detecting distant sources of airborne pollen for Poland: integrating back-trajectory and dispersion modelling with a satellite-based phenology. Sci. Total Environ. Nov 1;689, 109–125. https://doi.org/10.1016/j.scitotenv.2019.06.348.

Bruffaerts, N., De Smedt, T., Delcloo, A., Simons, K., Hoebeke, L., Verstraeten, C., Van Nieuwenhuyse, A., Packeu, A., Hendrickx, M., 2018. Comparative long-term trend analysis of daily weather conditions with daily pollen concentrations in Brussels, Belgium. Int. J. Biometeorol. 62, 483–491. https://doi.org/10.1007/s00484-017-1457-3.

Büntgen, U., Piermattei, A., Krusic, P.J., Esper, J., Sparks, T., Crivellaro, A., 2022. Plants in the UK flower a month earlier under recent warming. Proc. Biol. Sci. 289, 20212456. https://doi.org/10.1098/rspb.2021.2456.

Cariñanos, P., Guerrero-Rascado, J.L., Valle, A.M., Cazorla, A., Titos, G., Foyo-Moreno, I., Alados-Arboledas, L., Díaz de la Guardia, C., 2022. Assessing pollen extreme events over a Mediterranean site: role of local surface meteorology. Atmos. Environ. 272, 118928 https://doi.org/10.1016/j.atmosenv.2021.118928.

Casas-Castillo, M.C., Llabrés-Brustenga, A., Rius, A., Rodríguez-Solà, R., Navarro, X., 2018. A single scaling parameter as a first approximation to describe the rainfall pattern of a place: application on Catalonia. Acta Geophys. 66 (3), 415–424. https://doi.org/10.1007/s11600-018-0122-5.

Chen, H., Sun, J., Lin, E., Xu, H., 2020. Comparison of CMPI6 and CMPI5 models in simulating climate extremes. Sci. Bull. 65, 1415–1418. https://doi.org/10.1016/j.scib.2020.05.015.

Chuine, I., Cour, P., Rousseau, D.D., 1999. Selecting models to predict the timing of flowering of temperate trees: implications for tree phenology modelling. Plant Cell Environ. 22, 1–13. https://doi.org/10.1046/j.1365-3040.1999.00395.x.

Cordero, J.M., Rojo, J., Gutiérrez-Bustillo, A.M., Narros, A., Borge, R., 2020. Predicting the Olea pollen concentration with a machine learning algorithm ensemble. Int. J. Biometeorol. 65, 541–554. https://doi.org/10.1007/s00484-020-02047-z.

De Weger, L.A., Bruffaerts, N., Koenders, M.M.J.F., Verstraeten, W.W., Delcloo, A.W., Hentges, P., Hentges, F., 2021. Long-term pollen monitoring in the Benelux: evaluation of allergenic pollen levels and temporal variations of pollen seasons. Front. Allergy 2. https://www.frontiersin.org/articles/10.3389/falgy.2021.676176.

Emberlin, J., Detandt, M., Gehrig, R., Jaeger, S., Nolard, N., Rantio-Lehtimäki, A.J., 2002. Responses in the start of Betula (birch) pollen seasons to recent changes in spring temperatures across Europe. Int. J. Biometeorol. 46, 159–170. https://doi.org/10.1007/s00484-002-0139-x.

Emberlin, J., Smith, M., Close, R., Adams-Groom, B., 2007. Changes in the pollen seasons of the early flowering trees Alnus spp. and Corylus spp. in Worchester, United Kingdom, 1996-2005. Int. J. Biometeorol. 51, 181–191. https://doi.org/10.1007/s00484-006-0059-2.

Eyring, V., Bony, S., Meehl, G.A., Senior, C.A., Stevens, B., Stouffer, R.J., Taylor, K.E., 2016. Overview of the Coupled Model.Intercomparison Project Phase 6 (CMIP6) experimental design and.organization. Geosci. Model Dev. 9, 1937–1958. https://doi.org/10.5194/gmd-9-1937-2016.

Fitter, A.H., Fitter, R.S., 2002. Rapid change in flowering time in British plants. Science 296, 1689–1691. https://doi.org/10.1126/science.1071617.

Galán, C., Cariñanos, P., Alcázar, P., Domínguez-Vilches, E., 2007. Manual de Calidad y Gestión de la Red Española de Aerobiología. Servicio de Publicaciones, Universidad de Córdoba.

Galán, C., Smith, M., Thibaudon, M., Frenguelli, G., Oteros, J., Gehrig, R., Berger, U., Clot, B., Brandao, R., the EAS QC Working Group, 2014. Pollen monitoring: minimum requirements and reproducibility of analysis. Aerobiologia 30, 385–395.

Garcia-Mozo, H., Galan, C., Gomez-Casero, M.T., Dominguez, E., 2000. A comparative study of different temperature accumulation methods for predicting the start of the Quercus pollen season in Cordoba (south West Spain). Grana 39 (4), 194–199. https://doi.org/10.1080/00173130051084322.

Garcia-Mozo, H., Galán, C., Belmonte, J., Bermejo, D., Candau, P., Guardia, C., Elvira, B., Adela, M., Gutiérrez, M., Jato, V., Silva, I., Trigo, M.M., Valencia, R., Chuine, I., 2009. Predicting the start and peak dates of the Poaceae pollen season in Spain using process-based models. Agric. For. Meteorol. 149 https://doi.org/10.1016/j.agrformet.2008.08.013.

Gehrig, R., Clot, B., 2021. 50 years of pollen monitoring in Basel (Switzerland) demonstrate the influence of climate change on airborne pollen. Front. Allergy 2, 677159. https://doi.org/10.3389/falgy.2021.677159.

Grinn-Gofron, A., Strzelczak, A., 2008. Artificial neural network models of relationships between Alternaria spores and meteorological factors in Szczecin (Poland). Int. J. Biometeorol. 52, 859–868. https://doi.org/10.1007/s00484-008-0182-3.

Hirst, J., 1952. An automatic volumetric spore trap. Ann. Appl. Biol. 39 (2), 257–265. https://doi.org/10.1111/j.1744-7348.1952.tb00904.x.

Hoebeke, L., Bruffaerts, N., Verstraeten, C., Delcloo, A., De Smedt, T., Packeu, A., Detandt, M., Hendrickx, M., 2018. Thirty-four years of pollen monitoring: an

evaluation of the temporal variation of pollen seasons in Belgium. Aerobiologia 34, 139–155. https://doi.org/10.1007/s10453-017-9503-5.
IPCC, 2001, 2001. Climate change 2001: impacts, adaptation and vulnerability. In: McCarthy, J.J., OF Canziani, Leary, N.A., Dokken, D.J., White, K.S. (Eds.), Contribution of Working Group II to the Third Assessment Report of the Intergovernmental Panel on Climate Change. Cambridge University Press, Cambridge, UK, and New York, USA. No. of pages: 1032. Price:£ 34.95, ISBN 0-521-01500-6 (paperback), ISBN 0-521-80768-9.
IPCC, 2007. Summary for Policymakers. In: Solomon, S., Qin, D., Manning, M., Chen, Z., Marquis, M., Averyt, K.B., Tignor, M., Miller, H.L. (Eds.), Climate Change 2007: The Physical Science Basis. Contribution of Working Group I to the Fourth Assessment Report of the Intergovernmental Panel on Climate Change. Cambridge University Press.
IPCC, 2013. Climate Change 2013: The Physical Science Basis. Contribution of Working Group I to the Fifth Assessment Report of the Intergovernmental Panel on Climate Change [Stocker, T. F., D. Qin, G.-K. Plattner, M. Tignor, S. K. Allen, J. Boschung, A. Nauels, Y. Xia, V. Bex and P. M. Midgley (eds.)]. Cambridge University Press, Cambridge, United Kingdom and New York, NY, USA, 1535 pp. http://www.ipcc.ch/report/ar5/2.
IPCC, 2022. Climate Change 2022: Impacts, Adaptation, and Vulnerability. Contribution of Working Group II to the Sixth Assessment Report of the Intergovernmental Panel on Climate Change [H.-O. Pörtner, D.C. Roberts, M. Tignor, E.S. Poloczanska, K. Mintenbeck, A. Alegría, M. Craig, S. Langsdorf, S. Löschke, V. Möller, A. Okem, B. Rama (eds.)]. Cambridge University Press. Cambridge University Press, Cambridge, UK and New York, NY, USA, 3056 pp. https://doi.org/10.1017/9781009325844.
Izquierdo, R., Belmonte, J., Àvila, A., Alarcón, M., Cuevas, E., Alonso-Pérez, S., 2011. Source areas and long-range transport of pollen from continental land to Tenerife (Canary Islands). Int. J. Biometeorol. 55, 67–85. https://doi.org/10.1007/s00484-010-0309-1.
Izquierdo, R., Alarcón, M., Mazón, J., Pino, D., De Linares, C., Aguinagalde, X., 2017. Are the Pyrenees a barrier for the transport of birch (Betula) pollen from Central Europe to the Iberian Peninsula? Sci. Total Environ. 575, 1183–1196. https://doi.org/10.1016/j.scitotenv.2016.09.192.
Kasprzyk, I., Walanus, A., 2010. Description of the main Poaceae pollen season using bi-Gaussian curves, and forecasting methods for the start and peak dates for this type of season in Rzeszów and Ostrowiec Sw. (SE Poland). J. Environ. Monit. 12, 906–916. https://doi.org/10.1039/b912256g.
Laaidi, M., 2001. Forecasting the start of the pollen season of Poaceae: evaluation of some methods based on meteorological factors. Int. J. Biometeorol. 45 (1), 1–7. https://doi.org/10.1007/s004840000079.
Laaidi, M., Thibaudon, M., Besancenot, J.P., 2003. Two statistical approaches to forecasting the start and duration of the pollen season of Ambrosia in the area of Lyon (France). Int. J. Biometeorol. 48 (2), 65–73. https://doi.org/10.1007/s00484-003-0182-2.
Lee, K.S., Kim, K., Choi, Y.J., Yang, S., Kim, C.R., Moon, J.H., Kim, K.R., Lee, Y.S., Oh, J. W., 2021. Increased sensitization rates to tree pollens in allergic children and adolescents and a change in the pollen season in the metropolitan area of Seoul, Korea. Pediatr. Allergy Immunol. 32, 872–879. https://doi.org/10.1111/pai.13472.
Llabrés-Brustenga, A., Rius, A., Rodríguez-Solà, R., Casas-Castillo, M.C., 2020. Influence of regional and seasonal rainfall patterns on the ratio between fixed and unrestricted measured intervals of rainfall amounts. Theor. Appl. Climatol. 140 (1), 389–399. https://doi.org/10.1007/s00704-020-03091-w.
López-Orozco, R., García-Mozo, H., Oteros, J., Galán, C., 2023. Long-term trends and influence of climate and land-use changes on pollen profiles of a Mediterranean oak forest. Sci. Total Environ. 897, 165400 https://doi.org/10.1016/j.scitotenv.2023.165400.
Lops, Y., Choi, Y., Eslami, E., Sayeed, A., 2020. Real-time 7-day forecast of pollen counts using a deep convolutional neural network. Neural Comput. & Applic. 32, 11827–11836. https://doi.org/10.1007/s00521-019-04665-0.
Luedeling, E., Schiffers, K., Fohrmann, T., Urbach, C., 2021. PhenoFlex - an integrated model to predict spring phenology in temperate fruit trees. Agric. For. Meteorol. 307, 108491 https://doi.org/10.1016/j.agrformet.2021.108491.
Majeed, H.T., 2018. Study of the Meteorological Mechanisms Controlling Levels and Transport Processes of Airborne Pollen in the Atmosphere. PhD thesis.. Polytechnic University of Catalonia, Barcelona Tech, p. 166. https://doi.org/10.5821/dissertation-2117-123520.
Majeed, H.T., Periago, C., Alarcón, M., Belmonte, J., 2018. Airborne pollen parameters and their relationship with meteorological variables in NE Iberian Peninsula. Aerobiologia 34, 375–388. https://doi.org/10.1007/s10453-018-9520-z.
Makra, L., Matyasovszky, I., Deák, Á.J., 2011. Trends in the characteristics of allergenic pollen circulation in Central Europe based on the example of Szeged, Hungary. Atmos. Environ. 45, 6010–6018. https://doi.org/10.1016/j.atmosenv.2011.07.051.
Menzel, A., 2000. Trends in phenological phases in Europe between 1951 and 1996. Int. J. Biometeorol. 44, 76–81. https://doi.org/10.1007/s004840000054.
Menzel, A., Yuan, Y., Matiu, M., Sparks, T., Scheifinger, H., Gehrig, R., Estrella, N., 2020. Climate change fingerprints in recent European plant phenology. Glob. Chang. Biol. 26, 2599–2612. https://doi.org/10.1111/gcb.15000.
Monjo, R., Paradinas, C., Pórtoles, J., Gaitán, E., Redolat, D., Prado-López, C., Velasco, M., Russo, B., Jennings-Howe, A., David, L.M., Gabas, A., Matos, R., Stevens, J.R., Pouget, L., Vela, S., Ribalaygua, J., Silva, I.C., Telhado, M., Coelho, L., Baltazar, S., 2020. RESCCUE (RESilience to Cope with Climate Change in Urban arEas) EU Project - WP1 Data (1.0) [Data Set]. Zenodo. https://doi.org/10.5281/zenodo.3688402.
Moss, R.H., Edmonds, J.A., Hibbard, K.A., Manning, M.R., Rose, S.K., Van Vuuren, D.P., Meehl, G.A., 2010. The next generation of scenarios for climate change research and assessment. Nature 463 (7282), 747–756. https://doi.org/10.1038/nature08823.
Nakicenovic, N., Swart, R., 2000. Special report on emissions scenarios. Special Report on Emissions Scenarios, Edited by Nebojsa Nakicenovic and Robert Swart, pp. 612. ISBN 0521804930. Cambridge, UK: Cambridge University Press, July 2000, 1. https://archive.ipcc.ch/pdf/special-reports/emissions_scenarios.pdf.
Oh, J.W., 2022. Pollen allergy in a changing planetary environment. Allergy, Asthma Immunol. Res. 14, 168–181. https://doi.org/10.4168/aair.2022.14.2.168.
Piao, S., Liu, Q., Chen, A., Janssens, I.A., Fu, Y., Dai, J., Zhu, X., 2019. Plant phenology and global climate change: current progresses and challenges. Glob. Chang. Biol. 25, 1922–1940. https://doi.org/10.1111/gcb.14619.
Picornell, A., Maya-Manzano, J.M., Fernández-Ramos, M., Hidalgo-Barquero, J.J., Pecero-Casimiro, R., Ruiz-Mata, R., De Gálvez-Montañez, E., Del Mar Trigo, M., Recio, M., Fernández-Rodríguez, S., 2024. Effects of climate change on Platanus flowering in Western Mediterranean cities: current trends and future projections. Sci. Total Environ. 906, 167800 https://doi.org/10.1016/j.scitotenv.2023.167800.
Piotrowska-Weryszko, K., Weryszko-Chmielewska, E., Sulborska, A., Konarska, A., Dmitruk, M., Kaszewski, B.M., 2021. Amaranthaceae pollen grains as indicator of climate change in Lublin (Poland). Environ. Res. 193, 110542 https://doi.org/10.1016/j.envres.2020.110542.
Recio, M., Picornell, A., Trigo, M.M., Gharbi, D., García-Sánchez, J., Cabezudo, B., 2018. Intensity and temporality of airborne Quercus pollen in the Southwest Mediterranean area: correlation with meteorological and phenoclimatic variables, trends and possible adaptation to climate change. Agric. For. Meteorol. 250-251, 308–318. https://doi.org/10.1016/j.agrformet.2017.11.028.
Riahi, K., van Vuuren, D.P., Kriegler, E., Tavoni, M., 2017. The shared socioeconomic pathways and their energy, land use, and greenhouse gas emissions implications: an overview. Glob. Environ. Chang. 42, 153–168. https://doi.org/10.1016/j.gloenvcha.2016.05.009.
Rodríguez-Rajo, F.J., Grewling, L., Stach, A., Smith, M., 2009. Factors involved in the phenological mechanism of Alnus flowering in Central Europe. Ann. Agric. Environ. Med. 16 (2), 277–284.
Rodríguez-Solà, R., Casas-Castillo, M.C., Ho-Zhang, J.J., Kirchner, R., Alarcón, M., Periago, C., De Linares, C., Belmonte, J., 2022. A study on correlations between precipitation ETCCDI and airborne pollen/fungal spore parameters in the NE Iberian Peninsula. Int. J. Biometeorol. 66, 1173–1187. https://doi.org/10.1007/s00484-022-02267-5.
Rojo, J., Picornell, A., Oteros, J., Werchan, M., Werchan, B., Bergmann, K.C., Smith, M., Weichenmeier, I., Schmidt-Weber, C.B., Buters, J., 2021. Consequences of climate change on airborne pollen in Bavaria. Central Europe, Reg. Environ. Change 21, 9. https://doi.org/10.1007/s10113-020-01729-z.
Ruiz-Valenzuela, L., Aguilera, F., 2018. Trends in airborne pollen and pollen-season-related features of anemophilous species in Jaen (South Spain): a 23-year perspective. Atmos. Environ. 180, 234–243. https://doi.org/10.1016/j.atmosenv.2018.03.012.
Schramm, P.J., Brown, C.L., Saha, S., Conlon, K.C., Manangan, A.P., Bell, J.E., Hess, J.J., 2021. A systematic review of the effects of temperature and precipitation on pollen concentrations and season timing, and implications for human health. Int. J. Biometeorol. Oct;65(10), 1615–1628. https://doi.org/10.1007/s00484-021-02128-7.
Sicard, M., Jorba, O., Ho, J.J., Izquierdo, R., De Linares, C., Alarcón, M., Comerón, A., Baldasano, J.M., Belmonte, J., 2021. Measurement report: characterization of the vertical distribution of airborne Pinus pollen in the atmosphere with lidar-derived profiles – a modeling case study in the region of Barcelona, NE Spain. Atmos. Chem. Phys. 21, 17807–17832. https://doi.org/10.5194/acp-21-17807-2021.
Sofiev, M., 2019. On possibilities of assimilation of near-real-time pollen data by atmospheric composition models. Aerobiologia 35, 523–531. https://doi.org/10.1007/s10453-019-09583-1.
Sofiev, M., Siljamo, P., Ranta, H., Rantio-Lehtimaki, A., 2006. Towards numerical forecasting of long-range air transport of birch pollen: theoretical considerations and a feasibility study. Int. J. Biometeorol. 50, 392–402. https://doi.org/10.1007/s00484-006-0027-x.
Sofiev, M., Belmonte, J., Gehrig, R., Izquierdo, R., Smith, M., Dahl, A., Siljamo, P., 2013. A review of production, release, distribution and health impact of allergenic pollen. In: Bergman, K.-C. (Ed.), Sofiev, M. Springer, pp. 127–159. https://doi.org/10.1007/978-94-007-4881-1_5. Airborne pollen transport,.
Stach, A., Smith, M., Baena, J.C.P., Emberlin, J., 2008. Long-term and short-term forecast models for *Poaceae* (grass) pollen in Poznań, Poland, constructed using regression analysis. Environ. Exp. Bot. 62 (3), 323–332. https://doi.org/10.1016/j.envexpbot.2007.10.005.
Tang, J., Körner, C., Muraoka, H., Piao, S., Shen, M., Thackeray, S.J., Yang, X.I., 2016. Emerging opportunities and challenges in phenology: a review. Ecosphere 7 (8), e01436. https://doi.org/10.1002/ecs2.1436.
Valencia, J.A., Astray, G., Fernández-González, M., Aira, M.J., Rodríguez-Rajo, F.J., 2019. Assessment of neural networks and time series analysis to forecast airborne Parietaria pollen presence in the Atlantic coastal regions. Int. J. Biometeorol. 63, 735–745. https://doi.org/10.1007/s00484-019-01688-z.
Voldoire, A., Sanchez-Gomez, E., y Mélia, D.S., Decharme, B., Cassou, C., Sénési, S., Déqué, M., 2013. The CNRM-CM5. 1 global climate model: description and basic evaluation. Clim. Dyn. 40 (9–10), 2091–2121. https://doi.org/10.1007/s00382-011-1259-y.
Watanabe, S., Hajima, T., Sudo, K., Nagashima, T., Takcmura, T., Okajima, H., Ise, T., 2011. MIROC-ESM 2010: model description and basic results of CMIP 5-20 c 3 m experiments. Geosci. Model Dev. 4 (4), 845–872. https://doi.org/10.5194/gmd-4-845-2011.
Willmott, C.J., 1981. On the validation of models. Phys. Geogr. 2, 184–194. https://doi.org/10.1080/02723646.1981.10642213.

Wu, T., Li, W., Ji, J., Xin, X., Li, L., Wang, Z., Shi, X., 2013. Global carbon budgets simulated by the Beijing climate center climate system model for the last century. J. Geophys. Res. Atmos. 118 (10), 4326–4347. https://doi.org/10.1002/jgrd.50320.

Xiao-Ge, X.I.N., Tong-Wen, W.U., Jiang-Long, L.I., Zai-Zhi, W.A.N.G., Wei-Ping, L.I., y Fang-Hua, W.U., 2013. How well does BCC_CSM1.1 reproduce the 20th century climate change over China? Atmos. Ocean Sci. Lett. 6 (1), 21–26. https://doi.org/10.1080/16742834.2013.11447053.

Yukimoto, S., Adachi, Y., Hosaka, M., Sakami, T., Yoshimura, H., Hirabara, M., Mizuta, R., 2012. A new global climate model of the meteorological research institute: MRI-CGCM3: model description and basic performance. J. Meteorol. Soc. Japan Ser. II 90A, 23–64. https://doi.org/10.2151/jmsj.2012-A02.

Zhang, Y., Bielory, L., Cai, T., Mi, Z., Georgopoulos, P., 2015. Predicting onset and duration of airborne allergenic pollen season in the United States. Atmos. Environ. 103, 297e306. https://doi.org/10.1016/j.atmosenv.2014.12.019.

Ziska, L.H., Makra, L., Harry, S.K., Bruffaerts, N., Hendrickx, M., Coates, F., Saarto, A., Thibaudon, M., Oliver, G., Damialis, A., Charalampopoulos, A., Vokou, D., Heiðmarsson, S., Guðjohnsen, E., Bonini, M., Oh, J.W., Sullivan, K., Ford, L., Brooks, G.D., Myszkowska, D., Severova, E., Gehrig, R., Ramón, G.D., Beggs, P.J., Knowlton, K., Crimmins, A.R., 2019. Temperature-related changes in airborne allergenic pollen abundance and seasonality across the northern hemisphere: a retrospective data analysis. Lancet Planet. Health 3, e124–e131. https://doi.org/10.1016/S2542-5196(19)30015-4.